

Opus: An Integrated Simulation Model for
Transport of Nonpoint-Source Pollutants
At the Field Scale
Volume I, Documentation

Revised Edition, September, 2000

Note: This is a revised edition of Publication ARS-98, of the Agricultural Research Service, United States Department of Agriculture. It is intended as an electronically distributable version of the original document, with some updating revisions, and is not an authorized US government publication.

ACKNOWLEDGEMENTS

Methodology in this model borrows some material (as acknowledged herein) from earlier work in the EPIC model by Jimmy Williams, ARS Temple, Texas; from published research on various aspects of erosion relationships by George Foster; and the Century soil residue-nutrient model was modified for inclusion in Opus by Bill Parton, Colorado State University, Fort Collins, CO. We are grateful to Dr. Parton and his associates for their help. Opus also owes part of its origin to ideas not included in the CREAMS model due to time and other limitations. Much of the methodology for surface runoff dynamics benefited from the concurrent development of KINEROS (publication ARS-77) involving the contributions of David Woolhiser and David Goodrich, ARS, Tucson, AZ. Much of the testing was done with the assistance of Virginia Ferreira, ARS, with help from CSU students Walter Nicolli, Robert Flynn, and especially Fernando Pons.

CONTENTS

List of Symbols	4
1. Introduction	n
2. Characterizing the Physical System	
Specifying the catchment topography	
Abstracting the real catchment	
Implementing topography in the model	
Characterizing the soil profile	
3. Meteorological Processes	
Alternatives for weather simulation	
Simulation of a precipitation record	
Simulating occurrence of daily rain	
Simulating depth of daily rainfall	
Simulation of daily radiation and temperature	
Generating mean values for daily temperature and radiation	
Generating a stochastic record of daily temperature and radiation	19
Using recorded monthly weather data	
Reading recorded daily data	
Potential evapotranspiration	
Time distribution of PE_t	
Division of PE_t between plant and soil surface	
4. Flow and Transport by Soil Water	
Simulating flow of unsaturated soil water	
Simulating redistribution of soil water	
Simulating rain wetting profiles	
Simulating draintile or water table lower boundary	
Transport of soil heat	
Diffusion of soil heat	
Convection of soil heat with water	
Numerical implementation	
5. Surface-Water Flow Processes	
Simulation of runoff from daily rain data	
Simulation of runoff from breakpoint rainfall data	
Infiltration	
Treating a rainfall hiatus	
Infiltration through a surface crust layer	
Dynamics of surface water	
Kinematic wave flow	
Diffusive wave flow	
Estimation of hydraulic roughness	
Flow geometry relations	
Time step selection	
Irrigation flows	
Erosion and transport of sediment	
Sediment production for daily simulation	

- Distributed, dynamic erosion and sediment transport
 - Surface erosion and deposition
 - Concentrated flow erosion and transport
 - Erosion and deposition for mixed particle sizes
 - Evolution of flow geometry with erosion and deposition
- Impoundment storage
 - Routing of water through a pond
 - Routing of sediment through a pond
- Simulation of snow budget
 - Accumulation of snow
 - Simulation of snowmelt

6. Microbiological and Chemical Processes in Soil

- Transformations of nutrients
 - Nitrogen submodel
 - Phosphorus submodel
- Transformations of pesticides
- Pickup of chemicals by rainfall and runoff
 - Leaching of canopy chemicals
 - Leaching from surface residue
 - Routing chemicals during infiltration and runoff

7. Simulation of Plant Growth

- Growth model
 - Self-dependent growth
 - Growth limiting stresses
 - Water stress
 - Nutrient uptake and stress
 - Temperature stress
- Allocation of plant material
- Interaction of plant growth factors
- Discussion
- Example of plant growth simulation

8. Specifying Management Operations

- Lists of options
 - List of crops
 - List of tillage operations
 - List of chemicals
 - List of animal wastes
- Rotations and schedule of operations

9. Testing the Opus Model

- Testing, verification, and validation
- Tests of component processes
 - Daily weather model
 - Rainfall/runoff models
 - Soil water flow
 - Transport of solutes
- Opus demonstration example
 - Description of topography

Description of soil horizons
Management actions
Results
Summary

Literature Cited

List of Symbols

This list contains the most significant or most used symbols but is not exhaustive. Locally defined symbols may not be included but do not conflict with this list. A few of the symbols, to retain accepted usage in their respective discipline, may have more than one meaning (as indicated below) in different contexts. These symbols are used only when the meanings differ sufficiently to avoid ambiguity and when usages do not overlap. In addition, common abbreviations, such as N for nitrogen and C for carbon, are used in the text.

Units of measure throughout the text are abbreviated as follows:

m = meter	kg = kilograms
mm = millimeter	ha = hectare
l = liters	min = minutes
gm = grams	sec = seconds

Symbol	Definition	Units
a	cross-sectional area	m ²
A	surface area	m ²
A _p	pond area at h = 0	m ²
A _u	surface area contributing at the upstream point of a channel	m ²
c _h	conversion coefficient	ha-mm/l
C	concentration by weight	kg/kg
C _a	concentration of solute adsorbed to soil	kg/kg
C _p	phosphorus concentration	kg/l
C _w	concentration in liquid soil water	kg/l
C _s	volumetric concentration of sediment in surface water	
C _{sMX}	value of C _s at current conditions if steady; equilibrium C _s	
C _z	concentration of solute at time zero	kg/l
d	rate of transfer of suspended particles between soil surface and soil water	kg/m ² /min
d _{pr}	potential rill detachment rate	kg/m ² /min
d _r	actual rill detachment rate	kg/m ² /min
d _e	net rate of detachment or deposition	kg/m ² /min
D	diffusivity of soil water	m ² /min
D _T	soil thermal diffusivity	m ² /min
e _c	efficiency of mixing soil by cultivation	
e _r	plant respiration efficiency parameter	
E _p	daily potential plant-transpirable water	mm
E _{ps}	daily potential soil evaporation	mm
E _s	daily soil evaporation	mm
E _t	daily potential evapotranspiration	mm
E _t '	daily potential ET less intercepted water evaporation	mm
f	rate of infiltration	mm/min
f _b	content of soil carbon, by weight fraction	
f _c	fraction of clay in surface soil	
f _{NH}	NH ₄ factor in decay of plant residue	
f _{pw}	fraction of pesticide on plants subject to washoff	
f _{rm}	fraction of plant residue that is metabolic material	

Symbol	Definition	Units
f_{rs}	fraction of plant residue that is structural material	
f_{rz}	fractional content of soil organic residue by weight	kg/kg
f_s	fraction of sand in surface soil	
f_T	temperature factor in decay of soil residue	
f_W	soil water content factor in decay of soil residue	
$F()$	objective function to be minimized in numerical solution	
F_p	maximum fraction of surface area shaded by plants	
F_L	leaf area index: total leaf area divided by shaded area	
F_{LM}	index of potential maximum leaf area	
F_{LT}	index of total leaf area of all plants	
F_m	fraction of soil area shaded by mulch	
F_s	fraction of soil surface area shaded [mulch or plants]	
g	gravitational acceleration	m/sec ²
g_c	sediment transport capacity of surface flow	kg/m ² /min
g_s	actual sediment transport in surface flow	kg/m ² /min
G	soil effective capillary drive	mm
G_1	value of soil G for uncrusted surface soil	mm
G_e	value of G at wetting front given a crust or layered soil	mm
h	depth or height of surface water	m
h_o	Chapter 4: initial value of h_m at $t = t_o$	mm
\bar{h}	Chapter 5: normal surface water flow depth	m
\bar{h}	average height of superelevation of water table above draitiles	mm
h_m	maximum height of superelevation of saturation above draitiles	mm
H	total soilwater potential, $\psi - z$	mm
H_o	daily net effective radiant energy in equivalent water evaporation	mm
i	index subscript	
I	depth of infiltrated water for current event	mm
I_a	initial abstraction of water in SCS curve no. formula	mm
I_p	value of I at ponding or initiation of runoff from rainfall	mm
j	index of time increment in numerical expressions	
J	Jacobian tri-diagonal matrix	
k_o	dimensionless kinematic flow number: S_oL/h_o	
k_u	soil erodibility factor in the USLE regression formula	kg-hr/N/m ²
k_x	decay coefficient of carbon pool x in residue decomposition model	day ⁻¹
K	hydraulic conductivity of soil	mm/min
K_d	adsorption ratio for solutes in soil	l/kg
K_{OC}	base adsorption ratio [multiplied by soil carbon content to get K_d]	l/kg
K_s	effective saturated soil water conductivity; K at $\psi = 0$	mm/min
L_p	length of flow path of surface water	m
L_c	length of flow path through a channel	m
L_u	length factor in USLE formula for erosion	
m_p	content of pesticide in soil	kg/ha
m_{rL}	content of lignin in plant residue (in soil)	g/m ²
m_{rN}	content of nitrogen in plant residue	g/m ²
m_{rC}	content of carbon in plant residue	g/m ²
m_{rP}	content of phosphorus in plant residue	g/m ²
M	number of identical surface elements feeding into a channel [1 or 2]	
M_{lv}	plant dry matter in leaves and stems	kg/ha

Symbol	Definition	Units
M_m	soil mulch cover	kg/ha
M_p	total plant material (dry matter)	kg/ha
M_{pm}	total potential maximum plant material (dry matter)	kg/ha
M_s	mass of a soil layer	kg/ha
n	Chapter 5: Manning roughness coefficient Chapter 7: plant nitrogen content	kg/kg
N	number of basic runoff topologic units making up catchment	
p	probability function of continuous random variable	
p_i	probability of a discrete random variable	
P	total depth of daily or storm rainfall	mm
P_u	cropping practise factor in USLE formula	
q	flux per unit width of local surface water	m^2/min
q_e	flux of a water sink or source in soil column	mm/min
q_g	flux of soil water due to gravity	mm/min
q_i	inflow to a computational soil layer	mm/min
q_m	flux of soil water into saturated zone above draitile	mm/min
q_o	outflow from a computational soil layer	mm/min
q_p	peak rate of runoff	mm/min
q_s	volumetric flux of suspended sediment	m^3/min
q_u	flux of soil water due to capillary gradient	mm/min
Q	surface discharge	m^3/min
Q_{in}	inflow to a pond	m^3/min
Q_o	outflow from pond	m^3/min
Q_s	unit loss of sediment from watershed	kg/m^2
r	rainfall rate	mm/min
R	hydraulic radius of surface flow, a/ρ	m
\vec{R}	vector of R values along flow path	m
R_i	daily incoming solar radiation [one langley is $0.041868 \text{ mj}/m^2/\text{day}$]	langley
R_u	rinfall energy factor in USLE formula	ha-mm/N/h
s_w	parameter for soil water storage, in SCS curve number formula	mm
s_c	slope of soil water characteristic, $d\theta/d\psi$	mm^{-1}
S	slope of water surface	
S_o	slope of bed surface in direction of water flow	
S_u	slope factor in USLE formula	
t	time [units vary with process]	
T	temperature	$^{\circ}C$
T_K	Kelvin temperature	$^{\circ}K$
T_{min}	minimum daily temperature	$^{\circ}C$
T_{max}	maximum daily temperature	$^{\circ}C$
u	velocity of water	m/min
u^*	shear velocity	m/min
U_i	size 3 vector of cross-correlations in weather generation model	
v	local variable of integration, or coefficient	
v_s	particle settling velocity in water	m/min
V	volume of water	m^3
w	width of surface flow	m
w_s	water equivalence of a snowpack	mm

Symbol	Definition	Units
W	width of a distributed-flow hydrologic unit	m
x	distance along surface flow path	m
y _d	size of sediment particle	mm
y _s	spacing of parallel subsurface drains	m
Y	random variate, 0 to 1	
z	depth in soil measured from surface	mm
z _c	side slope (ratio of horizontal to vertical) of furrow or channel	
Z _t	total depth of soil profile modeled	mm
Z _r	depth of rooting	mm
α	Chapter 2: curvature parameter in soil-water characteristic function Chapter3: shape parameter for gamma probability distribution function [pdf]	
β	Chapter 3: scale parameter for gamma pdf Elsewhere: relaxation factor in numerical computations	
γ	specific weight of water	
γ _s	heat capacity of a soil particle	cal/cm ³ /°C
γ _w	volumetric heat capacity of water	cal/cm ³ /°C
δ()	iterative correction term	
Δ	slope of relation for saturation vapor pressure at mean air temperature	
ε	exponent in K(θ) relation	
θ	volumetric water content of soil	mm/mm
θ _r	residual soil water, a parameter in the soil characteristic function	mm/mm
θ _s	water content at natural saturation [ψ = 0]	mm/mm
Θ	normalized water content: (θ - θ _r)/ (θ _s - θ _r)	
κ _s	thermal conductivity of surface soil	mcal/cm
λ	pore-size distribution parameter	
v	kinetic rate partitioning coefficient	min ⁻¹
ξ	albedo of soil [or snow]	
ρ	wetted perimeter of surface water flow	m
ρ _b	wetted perimeter of the bottom of a furrow or channel	m
ρ _s	specific gravity of a soil sediment particle	
ρ _z	wetted perimeter of the sides of a furrow or channel [ρ = ρ _b + ρ _z]	m
σ	standard deviation of a random variable	
τ	bed shear due to flowing surface water	N/m ²
τ _c	critical shear at bed – shear at which sediment movement starts	N/m ²
τ _N	crop growth stress coefficient due to N deficiency	
τ _T	crop growth stress coefficient due to suboptimum temperature	
τ _W	crop growth stress due to insufficient soil water	
φ	modifying coefficient based on cropping effects, used in various formulas to estimate erosion detachment	
χ _i	residual vector in daily weather generation model	
ψ	soil water capillary pressure head (negative)	mm
ψ _b	air-entry parameter in soil retention characteristic	mm
ω	relative time weighting in numerical solution	

Opus, An Integrated Simulation Model for Transport of Nonpoint-source pollutants at the Field Scale: Volume I, Documentation

Roger E. Smith¹

1. Introduction

Models allow scientists to mathematically state what they have learned or believe about nature and natural processes. The familiar equations $F = ma$ and $e=mc^2$ are types of mathematical models. The advent of computers has given scientists the ability to represent knowledge and hypotheses of the interactions of several related processes. To the extent that the resulting model simulates nature, it allows the study of “what if” questions and the performance of certain limited experiments that might require years or centuries by physical experiments.

Several models have recently been produced that deal with the many of the interactive processes occurring in the water-based ecosystem of an agricultural field (SPAW, NTRM, CREAMS, and EPIC, to name a few). All such models are imperfect in some sense because of their limited knowledge of the various processes and their interactions. Although good theories may exist for parts of this system, at least under laboratory conditions, natural heterogeneities always confound to some extent the application of these theories to field conditions. Other processes may be only imperfectly understood or described, and empiricism or conceptual approximation may be required to represent some parts of the system.

Nevertheless, the need to study movement of potential pollutants from today’s chemically intensive agriculture has stimulated the building of and the use of models for agricultural hydrology and transport. In all cases, models are a compromise between scientific rigor and the practical limits as to the kind and extent of data that can reasonably be obtained for any model applications.

Opus (not an acronym) is offered herein as a potential improvement over currently available models for the processes of agricultural hydrology. It too is imperfect and has the limitations described above. However, Opus does overcome some of the weaknesses identified in several older generation models (Smith and Ferreira, 1989), and it has relatively advanced approaches to the simulation of water movement and chemical transport.

The purpose of Opus is to enable study of the effects of management and weather inputs on the movement of water and potential pollutants within and from a small catchment. Using the available physical and chemical information and the guidelines in the User Manual (Vol. 2), one can describe the plant parameters, the soil profile, and topography of a small simple catchment system; subject that system to either historical or statistically generated weather inputs and a management scheme; and select from a variety of output reports and simulation options to summarize the results of interest.

This volume I describes the theory and methodology used in the various processes simulated by the model, to provide the user a background for understanding the capabilities and limits of

¹ Now at Engineering Research Center, Colorado State University Foothills Campus, Fort Collins, CO 80523

the model. A second volume, the User manual, describes the required input data and the output options, and gives (where possible) a guideline for the selection of appropriate parameters for a given condition.

In addition to and in conjunction with water movement, Opus simulates the processes of sediment transport and chemical transport, and also the cycles of carbon, nitrogen, and phosphorus involved in microbial decay in the soil. Soil heat flow and crop growth are a part of the simulation. The model allows changes in these processes due to a wide variety of simulated management practices. Simulation of runoff, plant growth (if any), and soil water movement are always included; at the user's option, any of the other processes may be simulated concurrently.

The scope of Opus is limited to runoff areas that a) may be characterized by a single soil profile, b) have hydrologic complexity limited to first or second order channels networks, and are relatively symmetrical (as described below), and c) contain a single cropping system or plant cover regime. This does not mean that only one crop may be grown, or even one crop per year, but rather the entire area must be under the same cropping mix at one time. Opus is not limited to annual crops or to agricultural cropped areas, but can treat perennials and naturally vegetated catchments. Simulation periods of as little as a few days to many hundreds of years are possible.

The components of Opus were designed or selected to be of generally compatible precision. In other words, it was intended that all components be treated with a level of detail or sophistication appropriate to their influence on the outcome. [There have been, for example, sophisticated models of plant development which made grossly simple assumptions regarding soil water movement.] Nevertheless, the parts of this model do not necessarily reflect an equal level of understanding of all processes. There are necessarily some empiricisms in parts of the model; no model is entirely physically based, in the pure sense of the term.

Some parts or processes in Opus have been intentionally limited, as a choice between the complexity and the significance to most envisioned applications. For example, much of the thermodynamics of the soil freezing and snowmelt processes involves the latent heat of the ice/water system, which is not considered directly in Opus. The use of degree-day methods for estimating snowmelt is understood to be very approximate for a small area such as treated by Opus. Also, diurnal variations in the surface soil temperature are not treated: the average daily surface soil temperature is considered acceptable for study of long-term variations in profiles of soil temperature. This eliminates detail that may make a limited improvement in long-term simulation, and also eliminates the need for excessive detail in input data.

Opus allows several choices for simulation of the hydrologic component. The choice will mostly reflect the nature of the available rainfall data, plus the time scale of interest and the modeling objective. The hydrologic options are diagrammed in Figure 1. Implied in the variety of choices here is that the model is intended to have potential uses ranging from management to research. The available data should be appropriate for the intended modeling objective. Stochastically generated daily rainfall may be adequate for long-term study of alternate management schemes, but to look at details of hydrologic processes such as peak runoff rates and sensitivity of erosion to subtle management changes, one should have data on the rainfall intensity pattern. The physically-based simulation of infiltration and runoff is not possible without rain intensity data. Because these data are often recorded by noting the times and depths when the rate of accumulation changes, or the graph slope "breaks," these data are commonly and herein referred to as breakpoint rainfall data.

Much of Opus is original, but parts have taken advantage of process models developed by others. Included is a daily weather generation model which was taken with minor adaptation from the WGEN model of Richardson (1981). The evaporation potential model is based on that of Ritchie (1972). The daily runoff model is a modified version of the SCS² Curve Number (CN) model, with features from Williams (Smith and Willims, 1980) similar in the estimation of peak flow rates to the EPIC model (Williams *et al.* 1984). The soil erosion model accompanying the daily hydrology mode is from MUSCLE (Williams and Berndt, 1977).

The soil microbial system, including cycles of carbon, nitrogen, and phosphorus, is a daily time step version of the Century model (Parton, *et al.* 1988a,b). That model was verified by Parton for Opus to also include the addition of fertilizers and treat plant material additions from plowing under of crop material.

Opus operates on a basic daily cycle for most processes (illustrated in figure 2), with an annual and monthly accounting cycle for water balance components. There is also an annual time scale for management rotation, and smaller sub-time scales for soil and surface water flow and transport processes.

The remaining chapters in the volume detail the methodology used in the simulated processes and indicate how the processes interact. Volume 2, the User Manual, further describes the various options and gives detailed definition of the necessary input parameters.

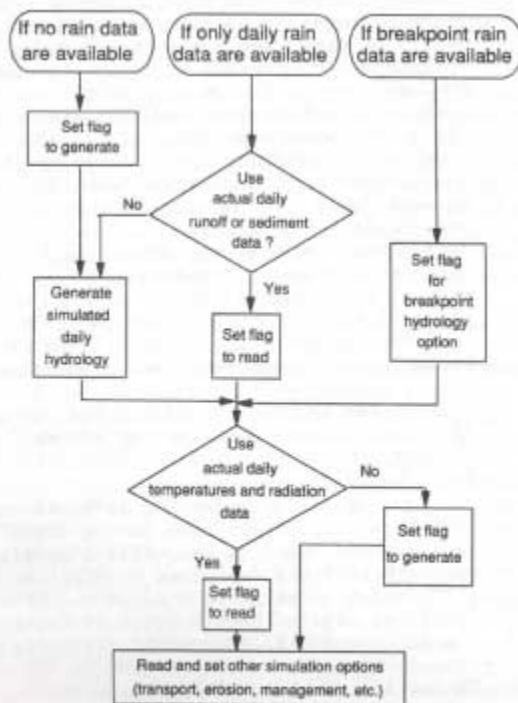


Figure 1. Options for method of hydrologic simulation available within the Opus program.

² Now the USDA NRCS

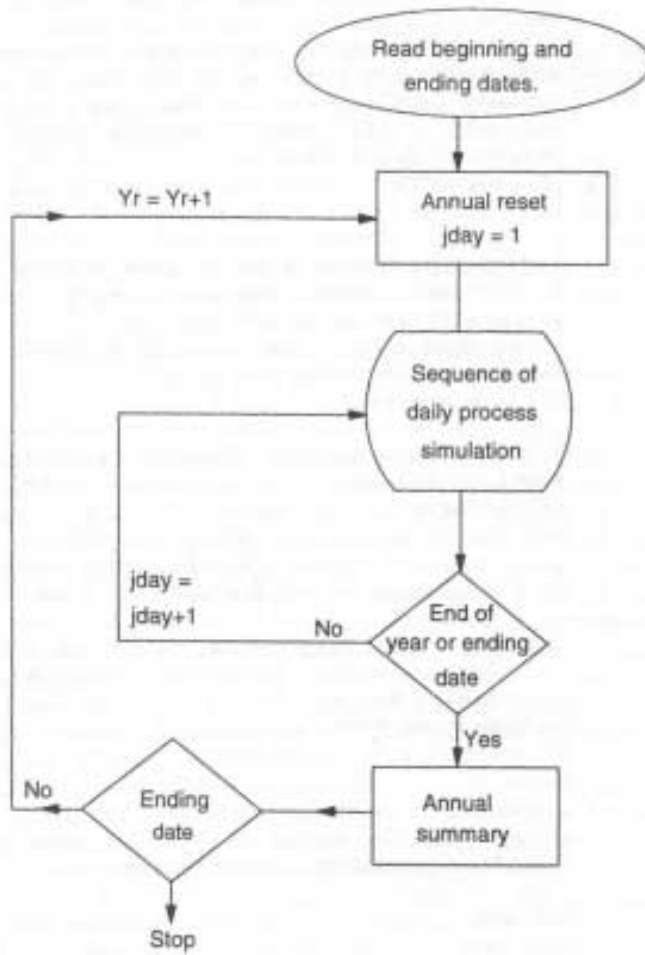


Figure 2. Basic daily and annual cycles of continuous simulation for Opus.

2. Characterizing the Physical System

Opus deals with the space within a small catchment, from the tops of the plants down to below the deepest roots. This is almost never a simple system, and any computer simulation begins with abstractions to describe the system in terms that allow reasonable approximation of the geometry. Two of the most important geophysical features of a catchment are the surface topology (slopes and flow paths of surface water) and the soil profile (including the soil hydraulic properties and how they vary with depth). This chapter indicates how these two key hydrologic components are described for Opus.

Specifying the Catchment Topography

Topography is a key factor in the transport of potential pollutants within and from a catchment area. Topography controls the paths of surface water flow, and influences the velocity of runoff from rainfall or irrigation. Finally, topography can enhance or inhibit the erosion of surface material.

Actual catchments are almost complex in shape at any level of detail. To simulate the surface hydrology without excessive amounts of input and computational detail, it is necessary to describe the area in geometrically simplified terms while retaining the features important for the hydraulics of surface water flow.

The daily hydrology option is a lumped time approximation, and is necessarily also a lumped-time method. Topographic information is useful in that approximation only in general measures, such as overall slope and flow length. Some of the following discussion will therefore not apply to that option because of the lumping involved. On the other hand, the infiltration based hydrology option (option 2) is relatively sensitive to topography, and the runoff is routed over the space of the catchment according to the specified geometry described below.

The method used in Opus to interpret the actual topography of a catchment is illustrated in figure 3. Surface water is not treated as a fully two-dimensional system, but flow is one-dimensional on a rectangular area, or else converges uniformly so that a one-dimensional equation may be used. Our present understanding of surface water hydrology indicates the following features need to be preserved: Catchment area, mean 'overland' flow path length, mean path length for channelized flows (where applicable), and slope of the mean flow path.

As shown in figure 3, the properties of each part of the flow path are preserved separately, with allowance for geometric simplification. This includes the preservation of non-uniform slope paths for simulation in hydrology option 2. As explained in the User manual, the slope profile is described by specifying the slope at each point along the profile where the rate of change of slope changes. This means that slopes at the beginning and end of a transition need to be given, and Opus interpolates slope changes uniformly between those limits. Uniform slope convergence is preserved by preserving the area and the width of the surface at the catchment divide.

Abstracting the Real Catchment. The basic topologic unit of the catchment in the model is limited to (a) a single distributed flow surface contributing uniformly along one side of a

first-order channel; (b) a matched pair of surfaces, one on each side of the first order channel; or (c) either (a) or (b) with a small area contributing directly to the upper end of the first-order channel. The total catchment then may be made up of several (or one) of these units, integrated by a second order receiving channel. The optional second order channel is assumed to take input from the N units uniformly along its length. This more complex arrangement can be used, for example, to explicitly simulate the organization of a field into terraces, with terrace channels contributing at the side to a receiving channel (illustrated below).

The structure outlined above can be used in varying forms and degrees of approximation to represent most topologies found in small catchments. The largest exception is strongly asymmetrical catchments, where a receiving channel or gully receives input from two sides which are significantly different in area. Opus can treat such cases only by forcing symmetry, or treating cases with very small inputs on one side as being essentially one-sided geometries. It was felt that explicitly treating asymmetries would double the computational effort without an appropriate return in precision.

An important feature in describing the flowpath topology for hydrology is the role that deep row furrows may play in controlling the path that water may take. Then, during part of the year when furrows may be removed by plowing, the water can take a different path across the field. In the case of contour plowing, the flow paths may be entirely different. This may change from year to year, or within the year. For this reason, Opus provides for alternate descriptions (sets of topological descriptive variables) for flow path geometries for the same field area. Case 1 describes the flow topology in the absence of furrows, governed solely by topographic slopes, and Case 2 describes the flow path topology when (and if) the flow is directed along a path determined by management defined furrow channels.

Figures 5 and 6 show the topology of two possible cases of flow path for one hypothetical field. Subscript 1 is for natural flow (case 1) and subscript 2 is for furrow-directed flow (case 2). In figure 5, flow is normal to the topographic contours, converging in this case towards the pond at the corner. In the method of Opus, the width of the abstracted flow surface at the upper end of the flow path is calculated from the field area and the user's estimate of the mean flow path down the slope. If the field is tilled to create case 2 as illustrated, flow goes from left to right along the furrow "microchannels". Convergence found in case 1 cannot occur under furrow flow control. The flow path is lengthened, and the path slope profiles are accordingly changed. The total change in elevation from top to bottom should be the same, and the parameters should preserve it. This may be stated mathematically, using subscripts corresponding to the two cases, as follows

$$\int_0^{L_1} S_1(x) dx = \int_0^{L_2} S_2(x) dx \quad [1]$$

where L_1 and L_2 are the total path lengths for cases 1 and 2 respectively, $S(x)$ is the slope profile in each case, and x is the distance along each path.

Figure 7 provides two other examples in which simplified hydrologic geometry is obtained from natural topography. In the upper example, because natural flow occurs normal to the contours, the field's actual shape should be distorted somewhat in the simplification, to preserve the actual mean flow-path length. This is because the flow direction, as shown, is at some angle to the (constructed) field border and is thus somewhat longer. Thus the simplified width is made slightly less than the topographic width to preserve the total area and mean path length. Another way to describe this is to say that the area is represented by a parallelogram of the given area.

In the lower case in figure 7, flow diverges as it moves from the hilltop toward the channels. This case could be simplified into two (triangular) planes, each contributing to the side of a different channel, with the two channels then joining. To preserve the area ABC and an estimated mean flow length (L_{p1}), the width of each abstracted surface is calculated as $W_1 = \text{area}/L_{p1}$. The mean width in this case would be less than the channel length, L_{c1} , but Opus apportions surface water input uniformly along receiving channel lengths. On the other hand, if the width so calculated is greater than L_{c1} , then converging flow is indicated, which is explicitly simulated in the surface water routing equations (chapter 5).

Terrace systems are common; figure 8 is a representation of an example terrace system. The Opus topological approximation requires that the individual areas of terrace drainage be represented as equal. Usually this is more or less accurate. Further, it is assumed that terrace spacings are identical. This is also commonly the case. Note in figure 8 the two sequential channels labeled L_{c1} and L_{c2} .

This case illustrates another important aspect of hydrologic topology. If the furrows are plowed closely parallel to the contours and thus follow the terraces, the major direction of significant runoff will be across the furrows and will occur only after a certain amount of surface water has been stored in the furrows. Opus recognises this case by investigating the furrow slopes: When slopes are negligible and runoff exceeds an estimated furrow storage (based on the furrow geometry specified), then overtopping is simulated, with runoff in the direction normal to the contours.

Implementing Topography in the Model Once the subject topology has been conceptually simplified, it must be described to the program. The minimum requirement for input to Opus is a description of the case-1 (unfurrowed) topology. This is sufficient for natural catchments or unplowed pastures or meadows. Case-2 topology is also described whenever (a) the initial furrow depth is significant or (b) management operations creating significant furrow depths are included in the operations menu (described below). Undisturbed fields where no management operations are used need only the case-1 topology described.

As noted above, from one to three elements make up the topological network through which water is routed. The first element is a flow surface across which flow is assumed to be uniformly distributed. This surface is not necessarily a plane or flat surface. It may represent one of two relative scales. At the smallest scale, where furrows or ridges are a significant part of the surface area (such as large terraces on severely sloping land), the first element may represent the sides of the ridges into a terrace and may be only a few meters in length. In this case, the furrow or swale between ridges becomes the first channel or the second element. Where ridges are close and numerous as in ordinary furrows, it is not recommended to represent fields in this detail, especially since it is unnecessary to route runoff over a flow path on the order of a meter or less in length.

For ordinary furrowed areas, it is preferable to use a larger scale approach and consider the first element to be an area with the furrows as microtopography. The input data for Opus allows the user to describe the flow geometry of the furrows without needing to treat each one as an individual channel in the routing sequence.

The basic catchment unit of an Opus field is made up of either one ($M=1$) or two ($M=2$) distributed flow elements, usually contributing to a channel (which is a central channel in the case of two surfaces). Provision is made for looking at a simple plot, so that a surface alone may

be treated without channel routing ($M=0$). The first channel is element 2. For simplicity the topology is characterized by symmetry. Thus there can be a number (N) of basic catchment units making up the total area, but they are equal. An additional upstream area (A_u) that contributes to the head of a channel (element 2) may also be designated as part of the basic unit. Figure 9 is a scheme of an example system for a case where $M=2$, there are 3 elements in the basic unit (one surface and two channels, not counting the area A_u), and four units ($N=4$) make up the total field.

If specified, the third element (the second channel) receives input uniformly distributed along its length, make up of the output from the N basic units. It also may have an upstream area A_u contributing separately. There are no multiples at this level: there is only one element 3 if any. Figure 10 shows the third element acting as a terrace outlet channel, such as in figure 8. In this scheme, there are no areas A_u and $M=1$.

Within the program, the flow length of each element is divided into computational increments. There can be from 3 to 20 such increments for any element flow path, depending on its length. The number of increments is generally taken as $\sqrt{2L}$, with L in meters.

Convergence of flow along the first element is found from the geometric parameters. As discussed below, the mean flow length L_p and the area of this element are required as input, and preserved in the model, and from this the mean width is calculated and compared with the length of the channel, element 2. If the channel length is equal or greater, then parallel flow is assumed. But if the channel length is smaller, and it is an unfurrowed condition, a convergence rate is calculated and used in the surface water routing. More details and examples of how to specify various conditions within this system are given in the User Manual.

Characterizing the Soil Profile

The soil profile is assumed to consist of one or more soil horizons, with each horizon differing from its neighbor in some significant manner. Such differentiation may consist of (a) differences in texture and thus in hydraulic characteristics, or (b) significant differences in nutrient or organic matter composition.

An Opus user may describe a profile made up of as many as 6 horizons. For computation purposes, the profile is subdivided systematically by the program into smaller computational increments, as illustrated in figure 11. The subdivision logic, which maintains the horizon boundaries, provides for a 10 mm upper increment, with increments generally increasing with depth. This follows the reasoning that changes are more rapid at the soil surface. Opus also internally subdivides the soil and surface into three portions for residue and nutrient dynamics: a litter layer at the surface, a microbiologically active upper region, and the lower portion of the soil which is less active. Presumably, these divisions separate microbiologically dissimilar environments. The active upper soil layer is assumed (Paron, et al. 1988b) to extend to about 200 mm.

The soil profile is an important hydrologic element because it is a porous medium through which much rain water flows, and also because it is the medium in which plants grow and extract water. Thus the soil horizons must be described in quantitative terms that relate to the soil's hydraulic characteristics as well as biological and chemical characteristics. For example, naming a certain horizon as "B1" or "A2" does not give information that can be used in

simulating its water holding and water moving capabilities. The same is true for the soil's name or color.

Whenever a soil is partially saturated, liquid water occurs in intergranular interfaces. Because of the strong surface tension of water, a significant negative pressure, locally continuous, is characteristic of the soil water at a particular water content. The lower the water content, the smaller the effective water surface radii at the granular interfaces, and the higher the negative pressure in the water. It is the gradient of this pressure, or soil water *matric potential*, that causes water to move in unsaturated soil. Most current management models however, treat soil-water movement using concepts of storage filling and draining.

Opus describes the relation of water content to matric potential with a flexible relation that is illustrated in figure 12. The general expression to describe the characteristic *retention relation* is

$$\Theta = \left[1 + \left(\frac{\psi}{\psi_b} \right)^\alpha \right]^{-\lambda/\alpha} \quad [2]$$

in which Θ is the normalized or scaled volumetric water content, defined as

$$\Theta = \frac{(\theta - \theta_r)}{(\theta_s - \theta_r)} \quad [3]$$

and ψ is matric water potential (mm),
 ψ_b is a parameter representing air entry potential (mm),
 α is a curvature parameter affecting the curve shape near ψ_b ,
 λ is a pore-size distribution parameter,
 θ is the volumetric water content,
 θ_r is residual water content, conceptually the soil water unextractable by capillary forces, and
 θ_s is water content at 0 matric potential.

This expression is similar to that of van Genuchten (1980)³, but relates directly to the Brooks and Corey (1964) relation, which contains parameters that represent physical concepts.

The companion relationship describing the unsaturated hydraulic properties of soils relates unsaturated hydraulic conductivity, K , to water content (and thence to matric potential). One robust expression for $K(\theta)$ is

$$K = K_s \Theta^\varepsilon \quad \text{or} \quad k_r = \Theta^\varepsilon \quad [4]$$

where k_r is relative hydraulic conductivity, K/K_s , and K_s is effective saturated hydraulic conductivity, or K at $\psi = 0$.

According to Brooks and Corey, the exponent ε may be approximated by relating to the pore size distribution parameter:

$$\varepsilon = (2 + 3\lambda) / \lambda \quad [5]$$

³ The parameters n and m of Van Genuchten are related to λ as $\lambda = n^*m$, and the parameter α of Van Genuchten is $1/\psi_b$ (except that α is usually in units of cm^{-1} rather than mm^{-1}).

In general, ψ_b is smaller for soils with larger pore sizes and is larger for soils with fine or very well distributed pore sizes. Similarly, parameter λ is small for soils with well distributed range of particle sizes and is large for soils with a very narrow range of particle sizes, such as sand or relatively clay-free silt. The value of K_s varies widely but follows a trend similar to λ , and depends more on the pore size and amount of clay in the soil.

To describe a soil horizon, therefore, Opus requires five major parameters: λ , θ_s , θ_r , ψ_b and K_s . To parameterize the model, however, instead of requiring a specification of θ_r , the user is asked for a value of water content at wilting point ($\psi = -15$ bars) which is often better known, and then θ_r may be found by using equations [2] and [3]. If a value of α is unknown, a default value of 5 is used. The selection of reasonable values for the hydraulic characteristics of a particular soil profile is an important task for the user of a physically-based soil flow simulation model such as Opus. When measurements are not available, Opus takes advantage of an extensive data set analysis done by Rawls et al. (1982) to give the user a survey of expected values for these parameters. This work has related the hydraulic characteristic parameters to the soil texture (sand, silt, and clay fractions) and soil porosity. The use of regression provides a way to estimate generally reasonable parameters in the absence of hydraulic experimental data. The regression relations which may be chosen for use in Opus are however not reliable for any given soil texture, and the data from which the regression relations were taken contained large variances in the parameter values for any given texture class. Experimentally determined soil data are far preferable. Other sources of such hydraulic data exist, including another texture class estimating table by Carsel and Parrish (1982), and a compilation of experimental data for sites in the US by Holtan et al. (1968). The role of hydraulic characteristic relations in simulating soil water movement is discussed in chapter 4, and was experimentally evaluated by Smith (1993).

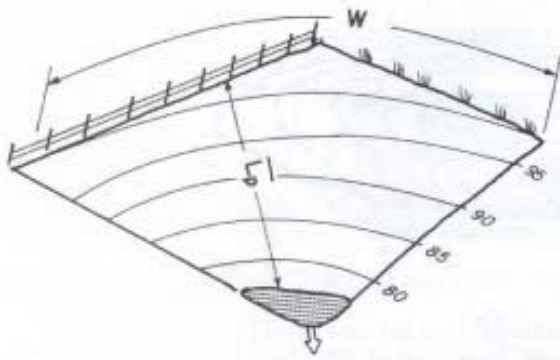


Figure 5. Example geometry of a convergent field with flow not controlled by furrows. A mean length is estimated as shown. The upper catchment width would be very large compared to the width at bottom, to represent convergence of flow lines toward the pond.

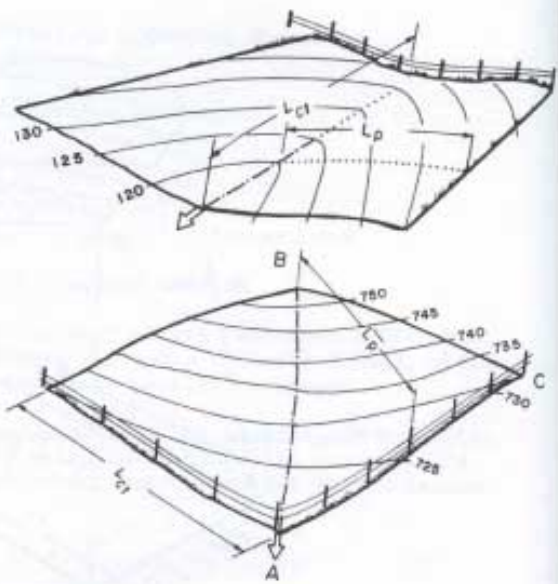


Figure 7. Two more examples of how surface flow is specified for fields of different topological characteristics. Divergent flow from the lower field is simulated by two different approximate planes. L_p is average flow length.

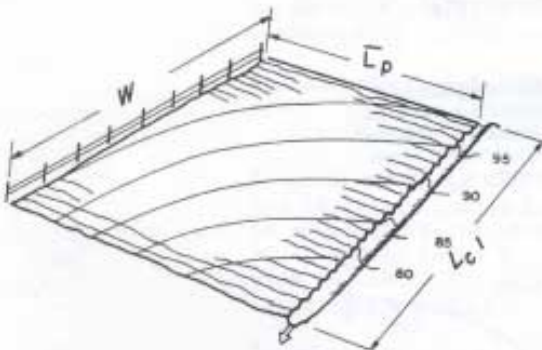


Figure 6. The same field as in figure 5, plowed to produce very different flow path. The width and length are both changed, but the area remains the same. Now a channel of length L_{cl} receives water from the furrows.

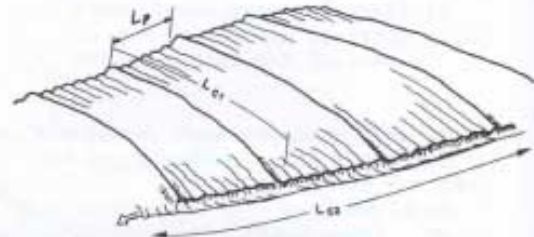


Figure 8. Representation of a typical terrace system. Terrace systems are common. Opus provides for a second-order channel (length L_{c2}) to collect flow from the terrace intercept channels (length L_{cl}).

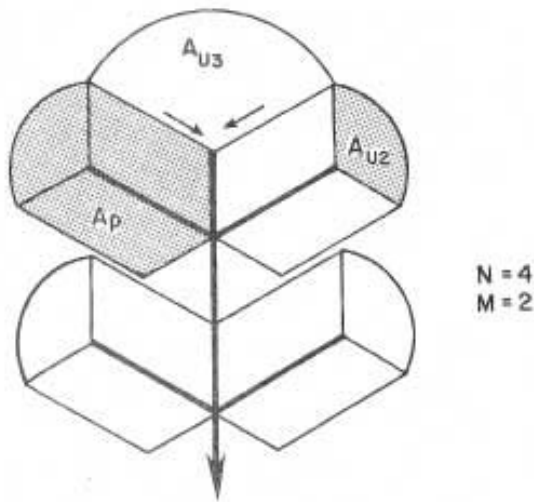


Figure 9. Example scheme of field topography. Opus limits complex geometries to symmetrical patterns, as shown here. Opus allows upslope areas that feed into the upper end of channels, here labeled A_{U2} for first-order channels and A_{U3} for second-order channels. The overall area is divided into four units, and each unit feeds from both sides of the channel ($M = 2$).

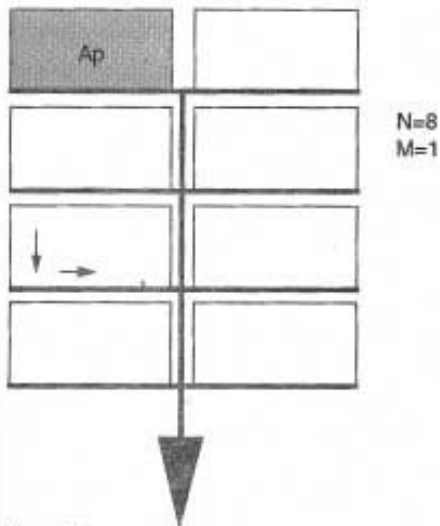


Figure 10. The terrace channel system as described for Opus, in simple geometry. Each of the eight units feeds to one side of its receiving channel ($M = 1$).

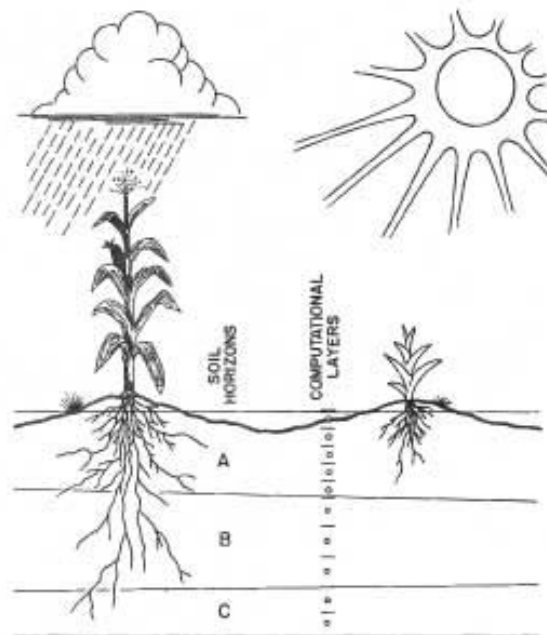


Figure 11. Soil horizons (e.g., A, B, C) are specified by the user and further divided into computational increments within the program.

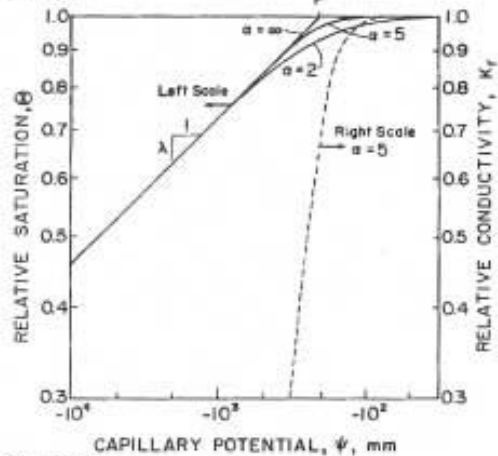


Figure 12. The unsaturated soil hydraulic characteristics are represented by an analytic expression that allows fitting to most soil types. Water content is normalized to relative saturation, θ , as shown in equation [3].

3. Meteorological Processes

The field unit simulated by Opus may be thought of as an ecosystem, including the plants and soil down through the root zone. In this conceptual framework, the meteorological processes are the driving ‘forces’ for this system, and the description of those processes is a crucial part of the simulation process. The meteorological variables that ‘drive’ or excite the system here include daily solar radiation (measured in langleys), daily maximum and minimum temperatures, and precipitation. These driver variables may be input or in some cases may be generated from input statistical parameters representing an analysis from local historical records.

Alternatives for Weather Simulation

Whenever available, records of daily maximum and minimum temperatures, daily radiation, and rainfall for a location are input to drive the simulation. The input format is described in the User Manual (Vol. 2). In practice, all required meteorological data may not be available for many locations for which simulation studies are desired, or may not have been collected frequently enough to allow physically sound simulations. Most likely the user will have only Weather Bureau summary data, perhaps including monthly means of temperatures, or will have only daily precipitation records, or will have some combination of these. So Opus has been designed to accept a variety of combinations of such actual records, including historical monthly averages of daily values of temperatures and radiation.

The weather generator model in Opus is built around a variation of the WGEN model (Richardson and Wright, 1984). This method requires as a minimum no additional recorded data, but falls back on a set of parameters which are provided in the form of parameter contour maps of the continental United States. The parameters may be determined for other areas provided a historical record is available. Opus also accepts monthly average temperatures and radiation values, and constructs its stochastic weather sequence to match those monthly values. Also, Opus allows the user to input a record of monthly mean pan evaporation values and a pan coefficient, as a surrogate for radiation values. Thus a variety of available data can be used in conjunction with the WGEN model to produce the necessary weather data for simulation.

Fundamental to the stochastic generator is the idea that these weather variables are intrinsically linked or correlated – that temperature and radiation variations from day to day should be related to each other and to the pattern of rainfall occurrence. The model can maintain both the statistical features of observed time series and the generally observed interdependencies between these weather variables.

The data-generating process and its assumptions are summarized below. In many cases, although daily temperatures and radiation values are available for a certain period of record, the user may choose to generate data when longer simulations are desired, instead of creating and handling massive files of input data.

Simulation of a Precipitation Record

When either daily or pattern (“breakpoint”) data for rainfall are available for the period of simulation, the data are given to the model in the form of a sequential data file. If such data are not available or if it is desired to simulate a period longer than the record, the statistical model of the occurrence and depth of daily rainfall may be used to generate rainfall sequences appropriate to the local climate. Note that only daily rainfall can presently be stochastically generated; breakpoint data if desired must be provided.

Simulating Occurrence of Daily Rain The occurrence of a rainfall day is modeled by WGEN as a Markov chain process of wet days and dry days. On rainfall or wet days, the amount is randomly distributed according to a two-parameter gamma distribution. A wet day is defined as one on which more than 0.25mm (0.01 inch) of rain falls. The following description is a summary of the WGEN methodology, and the reader is referred to Richardson (1981) or Richardson and Wright(1984) for a more complete discussion.

The Markov chain model of a binary process deals with transition probabilities, that is, the probability of a transition from a wet day yesterday (for example) to a dry day today. Let $p_i(w|d)$ represent the probability of a dry day following a wet day on day i . Then clearly,

$$p_i(w | w) = 1 - p_i(d | w) \quad [6]$$

and

$$p_i(d | d) = 1 - p_i(w | d) \quad [7]$$

Thus, specifying one each of these two complimentary pairs of probabilities, $p(d|w)$ and $p(d|d)$ fully defines the model. These probabilities change with seasonal climatic changes. With enough historical data, one can get a good picture of the change in transitions probabilities in some climates over periods as short as a few days to a week. For purposes of Opus, it considered adequate to define weather trends by month. Thus i is used in equations [6] and [7] as a monthly index, and the rainfall occurrence model requires a total of 24 parameters. Richardson and Wright (1984) have tabulated these parameters for many locations in the United States. These data are useful in simulating for ungaged areas, and are reproduced in the User Manual (Vol. 2).

Simulating Depth of Daily Rainfall The probability of the amount of rain, v , on wet days, $p(v)$, is estimated by a two-parameter function for gamma probability density:

$$p(v) = \frac{v^{\alpha-1} e^{-v/\beta}}{\beta^\alpha \Gamma(\alpha)} \quad , \quad v, \alpha, \beta > 0 \quad [8]$$

The parameters α and β are the parameters for shape and scale, respectively. Like the transition probabilities, they are assumed to vary by month at each location. Stochastic simulation of a daily amount involves generating, on ‘wet’ days, a uniform random variate Y : $0 < Y < 1$. Then Y is made to have the distribution

$$Y(v) = \int_0^v p(v) dv \quad [9]$$

which is inverted to solve for the precipitation value v satisfying this relation. When equations [8] and [9] estimate values of v less than 0.25mm, they are ignored and another value is produced. This procedure is consistent with the definition of a wet day given above.

Simulation of Daily Radiation and Temperature

Options chosen by the user, and the existence of records, will determine the method of simulating daily radiation and maximum and minimum temperatures. The basic model for the variation of these three variables (heretofore referred to as *weather variables*) assumes that in the mean they follow a sinusoidal annual variation, have a random variation about this mean pattern, are cross correlated, and are correlated with the wet/dry pattern of rainfall. This part of the model is also taken from the WGEN model, and is briefly described below. Richardson's methods have been modified to allow operation in the Celsius scale of temperatures. The changes to the basic model are described in the following sections.

Generating Mean Values of Daily Temperature and Radiation If monthly data on weather variables are provided, the simplest method for obtaining estimates of record-average daily values is to interpolate between monthly values, applying the monthly value at the middle of each month. This provides as smoothly changing value for each day. With this method, the values will change smoothly and daily values for a given calendar day will be the same each year. For some simulation objectives this may be satisfactory. For this as well as all other options, Opus applies a bias upward or downward for days that are dry or wet, respectively.

Generating a Stochastic Record of Weather Variables To obtain a more realistic sequence of daily weather variables, with or without dependence of recorded mean values, an autoregressive generation scheme may be used for each weather variable. Monthly mean values may be used as a control, but daily values are generated based on the model described by equations [6] through [9] above. Parameters are obtained from Richardson's parameter maps (provided in the User manual), for such parameters as the annual mean, the coefficient of the first fourier term, the annual mean variance, and the coefficient of the first fourier term of the annual variation of the variance. The values for generated daily radiation are shifted downwards on wet days.

Each of the daily values of T_{max} , T_{min} , and R_i are assumed to be related to their respective values yesterday in a autoregressive manner (Richardson, 1981):

$$x_i(j) = Ax_{i-1}(j) + B\chi_i(j) \quad [10]$$

where $x_i(j)$ is the vector of residuals of either $T_{max}(j=1)$, $T_{min}(j=2)$ or $R_i(j=3)$
 χ_i is a size-3 vector of independent random components, and
 A and B are 3x3 matrices whose elements define the serial and cross-correlation properties of these variables.

Richardson(1981) found that although means and standard deviations vary in space and time, it is a very acceptable approximation to assume constant values of the correlation matrices A and B . Opus uses such fixed matrices.

Since x_i is a residual value with mean 0 and standard deviation 1, the generated value of any given variable $v_i(j)$ is then found as

$$v_i(j) = \bar{v}_i(j) + x_i(j)\sigma_i(j) \quad [11]$$

where j indices are as defined above, and

\bar{v}_i is the mean value of v for day i , and
 σ_i is the standard deviation of v for day i .

The generation model distinguishes two sets of parameters for each location: one is for wet days and one is for dry days. Each set includes parameters for the annual mean and amplitude of the Fourier two-term series description of variable mean, plus a mean and amplitude for an annual Fourier sequence of the coefficient of variation of each. The coefficient of variation for temperature is transformed to a variance in Opus, because the coefficient of variation will not work accurately for mean values near zero (Celsius). The mean and amplitude for the coefficient of variation for daily radiation are assumed the same for all locations, based on an analysis of US locations.

Using Recorded Monthly Data When mean recorded data are available for any of the three weather variables, as indicated above, Opus adjusts generated values to have monthly means equal to the recorded means. The model uses recorded data in comparison with the Fourier means for each month, and determines a shift factor that keeps the long-term means of generated values consistent with the records provided. In almost all cases, despite the provision of the monthly means, Opus requires self-consistent values of the weather generating parameters.

Reading Recorded Daily Weather and Runoff Data When recorded daily data are available, an option in Opus allows the user to read in recorded daily weather values, as well as recorded values of runoff and sediment production from a catchment. A separate input file is used for this option, and the recorded data must coincide with the period of simulation required of Opus. No missing data is allowed. This option is provided for users who may be using Opus in connection with recorded plot or experimental catchment records, or may be wishing to focus on plant growth or other processes and use actual hydrologic information.

Potential Evapotranspiration

The values of temperature and radiation on a given day can be used to estimate the potential evapotranspiration (E_t) on that day. This is a measure of the energy available to evaporate and transpire water, and reflects the environmental conditions rather than the soil or plant status. The actual soil evaporation and plant transpiration will be less than this value and will reflect the other determinants. The method used in Opus to calculate E_t is a modified form of the equation used in CREAMS. It was developed by Ritchie(1972), starting from the relations of Penman. The equation and its components are

$$E_t = \frac{(1 + c_w)\Delta H_o}{\Delta + 0.68} \quad [12]$$

where c_w is a coefficient expressing effects of wind and humidity,
 Δ is the slope of the curve of saturation vapor pressure and mean air temperature, or

$$\Delta = 5304 \exp(21.255 - 5304/T_K) / T_K^2 \quad [13]$$

and T_K is daily mean Kelvin temperature.

The value of parameter c_w is 0.28 in Ritchie's equation, but Opus allows the user to modify it to account for local conditions. Conceptually, humid conditions reduce this factor and windy conditions increase it (Ritchie *et al.* 1976).

The second variable in the E_t equation is defined as

$$H_o = R_i (1 - \xi) / 58.3 \quad [14]$$

Where

ξ is the albedo of the field surface, and
 R_i is the incoming daily solar radiation, in langleys.

Equation [14] is an estimating algorithm for the daily net effective solar energy, H_o . The units of E_t are millimeters of water, and E_t can be thought of as a derived daily weather variable. Note that 1 langley = 0.0041868 $\text{mj}/\text{m}^2/\text{day}$.

The field albedo, ξ , is calculated as a combination of area-weighted factors for plant, mulch, snow, and soil covers. The albedo of dry surface soil is an input parameter. Snow albedo, if present, is presumed to vary with time, in days after snowfall (t_s), as follows:

$$\xi_{\text{snow}} = 0.4 + 0.5 \exp(-t_s / 12) \quad [15]$$

Soil albedo varies with normalized soil moisture content (Θ) and compares with the dry soil albedo (ξ_{ds}) as follows:

$$\xi_{\text{soil}} = \xi_{\text{ds}} (1 - 0.4\Theta^2) \quad [16]$$

Plant and mulch albedo is assumed constant at 0.23

Time Distribution of E_t Figure 13 schematically illustrates how Opus assumes the major weather variables to be distributed in time. Time distribution is important when computational time intervals, which may vary with the periods between rains, for example, occupy only part of a day. E_t for a day is assumed to occur during the non-rainy part of the daylight hours. Radiation is assumed to be distributed sinusoidally between dawn and dusk, as shown, on rainless days. From equations [12] and [14] this implies a sinusoidal distribution of E_t as well. A small time interval near dusk or dawn contributes considerably less incremental E_t than does an equal interval near noon.

Division of E_t Between Plant and Soil Surface For an estimated daily E_t , the soil and plant conditions determine the daily proportion expected to be evaporated from the soil surface or transpired through the plant leaves, or in winter, the amount evaporated from snow surfaces. In addition, some of the E_t will be used for evaporating water that is on the mulch or plant surfaces from intercepted rainwater. Such intercepted water has first access to E_t . The remaining part of

E_t is here referred to as E_t' , and is divided among soil surface evaporation, E_s , and plant transpiration, E_p .

Transpiration is estimated on the basis of the total area of leaves, related to the leaf area index, LAI. That portion of E_t' consumed by plants is estimated as

$$E_p = E_t' F_p c_s \quad [17]$$

Where F_p is relative surface area shaded by plants [0 to 1],
 c_s is relative effectiveness of plant cover as a function of leaf area index:

$$c_s = [1 + (2.5/LAI)^5]^{0.2} \quad [18]$$

Leaf area index is defined as the ratio of the total leaf area to the ground area projection or shade under the plant. Equation [17], through the factor F_p , also accounts for sparse plant cover. The value of c_s can vary from 0 to 1. Further discussion of the plant use of water is found in Chapter 7.

Soil evaporation is estimated from the portion of soil surface not shaded by plants or litter (mulch). The total shaded area includes both plants and litter, and is estimated as

$$F_s = F_p + (1 - 0.5F_p) F_m \quad [19]$$

Where F_m is the relative area covered by mulch, estimated based on mulch loading in kg/ha. The relative amount of E_t' assigned to soil evaporation is controlled by the soil-water content in the near surface region. Without this latter control, the potential soil evaporation, E_{ps} , is

$$E_{ps} = E_t' \exp(-1.2F_s) \quad [20]$$

Soil evaporation proceeds in the two-stage process assumed by Ritchie (1972) and used in CREAMS (1980). The first stage is short and proceeds at the potential rate (E_{ps}) based on micrometeorologic conditions. The second stage represents soil-limited evaporation, and the rate is reduced proportionally to the square root of time, provided soil water can be moved toward the surface at this rate. This process reduces the actual soil evaporation (E_s) below the potential value E_{ps} .

From equations [18] through [20], $E_s + E_p$ do not always necessarily sum to E_t' . If the sum is greater, the deficit is allocated to keep the sum at E_t' . Of course the plant may not be able to transpire its potential if the soil water is limited. If $E_s + E_p$ is less than E_t' , no adjustment is required.

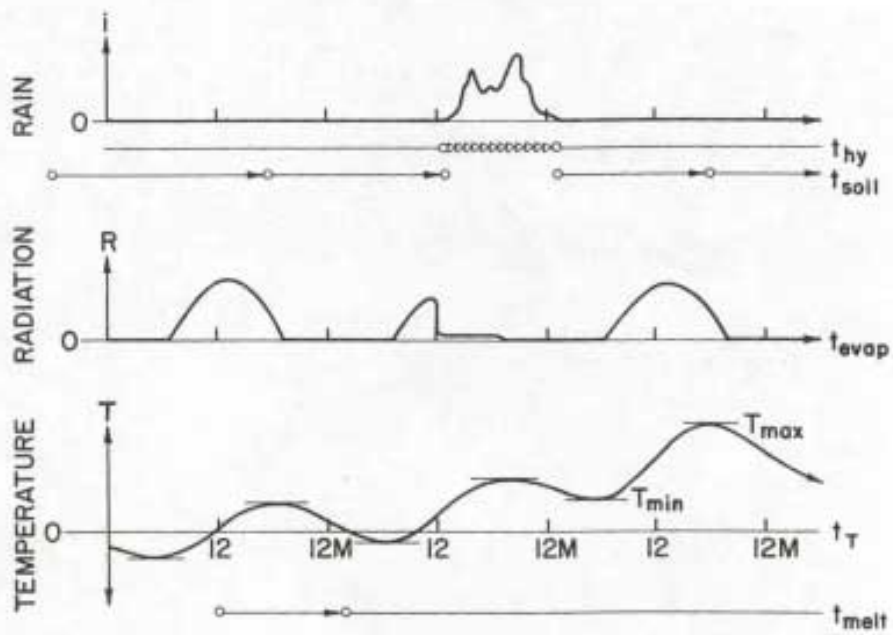


Figure 13.
 Time distribution of major weather variables in Opus.
 Radiation is assumed to vary with solar angle as shown, and
 temperature is assumed to follow a daily sinusoidal cycle.
 Radiation is reduced during a rain, and rain also reduces the
 daily maximum temperatures.

4. Flow and Transport by Subsurface Water

Soil-water dynamics involves most of the precipitation falling on the agricultural catchment and is thus a key element in the water transport of pollutants, both directly and indirectly. The zone of unsaturated flow extends from the soil surface down to the water table. In most cases, the solution region in Opus will extend to only a short distance below the bottom of the deepest roots, but the lower boundary will still be affected by the proximity of the water table. In the case of artificial drainage, the solution region will extend to the lower boundary control, which is the tile drain depth.

Simulating Flow of Unsaturated Water

Opus uses Richards' equation to describe water flow in the unsaturated soil profile. This mathematical expression is based on a dynamic, one-dimensional form of soil water conservation, expressed as

$$\frac{\partial \theta}{\partial t} + \frac{\partial q}{\partial z} = q_e \quad [21]$$

where θ is volumetric soil water content,
 t is time (minutes),
 z is depth from the surface (mm),
 q is soil water flux, (mm/min), and
 q_e is local inflow or loss (mm/min/mm).

The value of q is assumed to be described by Darcy's law, which relates flux to gradient of total potential, H :

$$q = -K \frac{dH}{dz} \quad [22]$$

where K is hydraulic conductivity (mm/min) and H is $\psi - z$ (capillary plus gravitational potential). From this definition of H ,

$$\frac{dH}{dz} = \frac{d\psi}{dz} - 1 \quad [23]$$

Richards' equation describes the simple unsaturated, one-dimensional vertical flow of water, and neglects the counterflow of air, among other assumptions. It does not attempt to account for soil-water vapor movement of water involving thermodynamics, nor does Opus attempt to simulate the thermodynamics of freeze-thaw cycles during winter. As discussed later, however, basic transfer of soil heat is simulated. These assumptions are not considered to be restrictive in the larger context of uncertainty within which Opus is envisaged to apply.

Simulating the Redistribution of Soil Water There is an analytic solution scheme for equations [21] + [24], but it requires particular assumptions on the soil characteristics and the boundary and uniformity conditions that are generally unrealistic, and here a numerical scheme is used.

The subdivision of the soil profile has previously been referred to. Each numerical layer is assigned a node in its center, between which gradients are calculated.

In numerical solution, it is important to properly characterize the effective mean soil properties between numerical layers, and to retain a suitable local value of the highly nonlinear relation of K to ψ or to θ . There is another challenge in correctly characterizing the flow and soil characteristic values across horizon boundaries. Haverkamp and Vauclin (1979) have summarized and compared several published techniques for $K(\theta)$ averaging within numerical solutions.

For Opus, with relatively large z increments, especially at greater depths, the problem is more acute than for research models that may use elements of only a few mm in thickness. One method of improving the solution is to take equations [22] and [23] together and consider q to be made up of two flux components, q_d and q_g , corresponding to diffusive and gravitational gradients, respectively:

$$q = q_d + q_g = -K_d(\theta) \frac{d\psi}{dz} + K_g(\theta) \quad [24]$$

The different subscripts on K represent potentially different ways of estimating the inter-layer values that are appropriate. K_g may be estimated, for example, by using the θ or ψ value of the upper increment, from which gravitational flow originates. There are certain cases, however, where for mass balance the two estimates need to be equal.

For flux caused by capillary gradients, or diffusive flux, an efficient interlayer estimate for K_d ($i, i+1$) can be derived by assuming, reasonably, that ψ varies uniformly between points z_i and z_{i+1} . While $d\psi/dz$ will be continuous and uniform between nodes within a soil or between two horizons, $d\theta/dz$ will be discontinuous at horizon interfaces. This is illustrated in figure 14. Since $K(\theta)$ is a relatively simple relation (equation [14]), the net K is calculated as the first moment of $K(\theta)$ over the computational interval within each horizon. When soil types change at an interface, we define θ_{bj} as the water content on the j side of interface b , for $j = i$ or $i+1$. The first moment of $K(\theta)$ between i and $i+1$ is

$$K_d(i, i+1) = \frac{1}{(\theta_i - \theta_{b,i})} \int_{\theta_{b,i}}^{\theta_i} K_i(v) dv + \frac{1}{(\theta_{b,i+1} - \theta_{i+1})} \int_{\theta_{i+1}}^{\theta_{b,i+1}} K_{i+1}(v) dv \quad [25]$$

With the soil's relation for $K(\theta)$ characterized simply as described in chapter 2, the solution of equation (25) is relatively straightforward.

Using the conceptual division of q from equation [24], equation [21] becomes

$$s_c(\psi_i, \bar{t}) \frac{\partial \psi_i}{\partial t} = \frac{\partial}{\partial z} \left[K_d \frac{\partial \psi}{\partial z} - K_g \right]_i + q_{ei} \quad [26]$$

where s_c is the slope of the hydraulic characteristic $d\theta/d\psi$ applicable at i and time t . Importantly, this value should represent the chord slope from the point on the characteristic at time $t - dt$ to the point at time t . This must be updated in the implicit solution iteration so that mass is conserved.

The first step in the solution procedure in Opus is a time step selection. This is accomplished by calculating q in equation [24] for flow between all nodes based on current conditions. A time step is chosen so as to limit the net rate of change of θ within a finite element. Critical conditions that are examined in this step include (a) drying to near θ_r at the surface, (b) potential (artificial) gradient reversals that would occur for local conditions with large differences in q .

As indicated above, values of s_c are chosen as chord slopes, and are updated during the solution. Estimates of K_d and K_g are found at the beginning of the time step and are not iterated. The nonlinear nature of the $\theta(\psi)$ and $K(\psi)$ relations and their reversal of curvature require the use of a relaxation technique, and the relaxation factor is allowed to grow after several iterations, if required. Because of the large variety of soil conditions and severe nonlinearities, the time steps can vary as needed between 0.01 and 1440 minutes (one day).

Richards' equation is not solved during inflow from a storm when the infiltration model hydrology option is used. During this period, rather, the net inflow to the soil is calculated, and put in with creation of a realistic wetting profile. When rains occur at a low rate, the profile is elongated since the surface soil will not have reached saturation. Thus the upper boundary condition is most often a negative flux representing soil evaporation. For small amounts of slow snowmelt, the upper boundary flux can be positive.

Local inflow values q_c are negative when there is local root water extraction. The total root-water use is distributed according to the water potential seen by the plant at each level, which is proportional to $\psi_i - z_i$. Continuous accounting is made of the root zone available water. On a daily basis, this is compared with the water demand of the plant and with the estimated wilting point potential, to limit plant uptake in response to stress. When the surface soil potential reaches -15 bars, the upper bound for evaporative flux is moved to the next lower increment.

The lower boundary potential, ψ_L , for equation [26], as indicated above, is located either at two computational nodes below the lowest root depth, or at the level of drains when simulated. In the former case, ψ_L is allowed to rise at the boundary in a kinematic manner when a θ "wave" passes below the roots (a positive $d\psi/dz$). Conversely, ψ_L may decrease as this wave passes out of the root zone. In no case is ψ_L allowed to decrease below the value that represents a hydrostatic condition relative to the water table. Periods of drought, or large root-zone demands, can cause upward movement to the roots in the soil below the root zone, but not to the extent to draw water from the water table. If draitiles are simulated (described below) the unsaturated zone solution includes the possible partly saturated region above the tile level.

In model simulation, soil water is redistributed over periods of about 1 day. When a day includes a storm, the soil water simulation period will go to the beginning of the storm, and the next period will start at the beginning time, with the storm input added as described below. If there is no rain, the simulation interval will go to 6:00 pm. This is an arbitrary division point for nonstorm days. Especially for complex storms, the time scale of patterns of surface flux during a storm is felt to be unnecessarily detailed for the purposes of Opus. In any case, for the daily hydrology option, input flux rate information is not available.

Simulating Rain Wetting Profiles When runoff occurs, saturation of the surface soil must have occurred, and conversely for small storms, the saturation will reflect the mean rainfall rate as a

fraction of K_s . Thus a first-order estimate of the resulting wetted-soil profile can be made as a step wave of depth equal to the infiltrated amount divided by $(\hat{\theta}_0 - \theta_i)$, where $\hat{\theta}_0$ is the estimated surface saturation, and θ_i is the pre-storm value of θ at each depth. In the model, the surface saturation is estimated and, starting at the surface, layers are filled to this value until the infiltrated amount has been exhausted. For smaller storms, a characteristic rainrate, $r_u < K_s$, is used in the relation for $K(\theta)$, inverted to become $\theta(K)$ which is used for $\theta_o(r_u)$.

The relative efficiency of the method described here, using relatively large z increments, is exemplified in figure 15. The initial condition profile is shown as a dashed line. The method of Opus is compared with a precise, fine-mesh solution by a fully implicit modified Crank-Nicholson method (Smith, 1970). Given the vast difference in increment scale, the Opus method is quite a faithful simulation compared to the fine-scale solution, which takes about two orders of magnitude more computation time. What is not demonstrated here is that the use of more common K -averaging schemes and standard numerical methods such as linearization would not produce an acceptable approximation to the behavior of equation [21].

Simulating Draintiles at the Lower Boundary

When draintile management methods are used in areas of relatively high water tables, the action and effect of the draintiles are important lower boundary controls on the unsaturated flow region. In Opus, the flow in the drains and their effect on the unsaturated region is simulated through an analytic expression for superlevation due to draintiles based on work of Bouwer and van Schilfegaarde (1963). Figure 16 illustrates the approach used to link the saturated and unsaturated regions. The superlevation of the water table above the drains is assumed to describe a half-ellipse in shape. Thus the mean superlevation of the water table is taken as the positive head at the drain level, h_N , and is a fixed fraction $\pi/4$ of the maximum superlevation, h_m . The formula assumes the flux through the draintiles is a quadratic function of h_m . The unsaturated flux from above, $q(z,t)$ at level h_m , can be assumed constant over the period Δt of interest (usually the same as the dt of the numerical solution). This input is termed q_m and is found in the unsaturated flow solution. The water balance then at the lower part of the soil profile can be written as

$$\phi \frac{dh_N}{dt} = q_m - q_d(h_N) \quad [27]$$

in which

$$\begin{aligned} q_d & \text{ is drain discharge (mm}^3/\text{mm}^2/\text{min), and} \\ \phi & \text{ is effective soil porosity in the drain region.} \end{aligned}$$

From Bouwer and van Schilfegaarde (1963) we use Houghoudt's quadratic equation for q_d , which may be written

$$q_d = c_a h_m^2 + c_b h_m \quad [28]$$

in which c_a and c_b are geometrically calculable parameters as follows:

$$c_a = \frac{4K_s}{y_s^2} \quad [29a]$$

$$c_b = \frac{8K_s z_e}{y_s^2} \quad [29b]$$

The quantity z_e is a function of the distance below the drains to a limiting interface, and is internally calculated in Opus based on the graphical results from Bouwer and van Schilfegaarde (1963).

Since equations [27] and [28], through the assumption of an elliptic surface can be cast in terms of the mean head h_N [= positive value of ψ] at the drains, they form a lower boundary expression for this value when there is superelevation. The quadratic expression resulting is partially linearized by expressing $(h_N^j)^2$ as $h_N^{j-1}h_N^j$, where j is the time index. Very little accuracy is lost in this method, because in almost all cases, the second-order term is 2 orders of magnitude smaller than the first-order term. The linearization allows the equation to be combined into the tri-diagonal solution matrix of the unsaturated flow equation solution.

Flow toward the active roots and soil evaporation can cause the water table for some cases to drop below the drain level. Opus treats this condition as it does a profile without drains. The relation between water deficit below the drains and the negative H at the drains is assumed to be equal to that of a soil column at equilibrium. This varies as necessary for the balance of volume at level h_N . When the water table again rises to the drain level by flow from above, the boundary condition reverts to the drain equation. Use of a fixed but very small positive value of s_c for all $\psi > 0$ allows Opus to solve for positive as well as negative matric potential values.

Transport of Soil Heat

The biological processes in the soil are sensitive to temperature, so it is important to simulate the temperature changes throughout the root zone profile during the year. Both plant growth and microbial activity are temperature dependent, and these processes are involved in pesticide degradation as well as nutrient cycling and residue decomposition. Although large changes occur through the day in the near surface soil, due to air temperature as well as solar radiation, Opus focuses on the variation in mean daily temperatures.

Heat moves through the soil by convective transport with water and by diffusion from temperature gradients caused by gain and loss of heat at the soil surface. In Opus, heat convection is treated in a manner similar to the movement of water, with thermal redistribution is treated as diffusion.

Diffusion of Soil Heat The soil profile is a significant heat storage mass, and changes in daily surface air temperature cause diffusion of heat into and out of the soil. The general one-dimensional equation for heat diffusion is

$$\frac{\partial T}{\partial t} = D_T(\rho, \theta) \frac{\partial^2 T}{\partial z^2} \quad [30]$$

with boundary conditions used as follows:

$$\begin{aligned} T(0,t) &= T_o, \quad 0 < t < 1440 \text{ min, and} \\ T(L,t) &= T_{av} \end{aligned}$$

where L is the lowest depth of simulation, and

- T is temperature, °C,
- D_T is thermal diffusivity of the soil, mm^2/min ,
- t is time in min.,
- z is depth from the surface, mm,
- ρ is the soil density, g/cm^3 ,
- T_{av} is the average annual temperature.

The initial condition used depends on the time of year at which the simulation starts, and maintains a smooth temperature gradient from the expected daily temperature at that time of year at the surface to the fixed lower bound temperature. Soil thermal diffusivity is theoretically a function of the mineral composition, the shape and orientation of the soil particles, and the water content (de Vries, 1966). Mineral thermal diffusivity is computed following a procedure from de Vries, based on soil clay content, and assuming randomly shaped particles. The water content is assumed constant (but non-uniform) over the period of computation. Thus D_T can be determined for each soil layer, and the difference form of equation [30] is quickly solved at each time interval with a direct Gauss-Seidel method. T is found not at the layer nodes, but at the layer interfaces, and node temperatures are easily determined by averaging. The use of the fixed annual average T at the lower bound is a reasonable assumption for all but shallow depths of simulation. Although equation [30] could be solved through the day to simulate diurnal excursions of near surface temperatures, it is not felt to be necessary for most of the objectives of Opus.

Convection of Soil Heat with Water Heat may be brought into the soil with the influx of water, and heat may be transported within the soil as soil water moves. Complete thermal mixing is assumed within each incremental layer of the flowing water, and initial soil-water temperature is assumed to be in equilibrium with the soil mass. The general convective heat balance may be written as

$$\gamma_w \frac{\partial(qT)}{\partial z} + \gamma_w \frac{\partial(\theta T)}{\partial t} + \gamma_s m_s \frac{\partial T}{\partial t}$$

where m_s is the soil mass. One may alternatively write an ordinary differential equation for each finite difference volume, treating it as a storage with complete mixing, to produce a simpler form for solution as follows:

$$\gamma_w [T_i q_i - T_o q_o] = \frac{d}{dt} [(\gamma_w V_w + \gamma_s V_s) T_o] \quad [31]$$

in which

- T_i is temperature of inflow water, °C,
- T_o is temperature of layer and outflow water,
- γ_w is volumetric heat capacity of water ($\text{cal}/\text{cm}^3/^\circ\text{C}$)
- V_w is volume of incremental layer (cm^3),
- γ_s is volumetric heat capacity of the soil ($\text{cal}/\text{cm}^3/^\circ\text{C}$),
- V_s is the volume of soil in the incremental layer
- q_i is the water influx (cm^3/min),
- and q_o is the water outflow (cm^3/min).

The equation is applied to a unit area, so that the volumes reduce to water contents in cm. This form of the equation assumes mixing within each layer, which is why T_o is used for both the internal and the outflow temperature. The left side of the equation is the net input of heat, and the right side is the change of heat in the layer. The general solution to this linear differential equation may be written as

$$T_o = T_i + (T_{oz} - T_i) \left[\frac{V_{wz} + bV_s + \Delta V}{V_{wz} + bV_s} \right]^{\frac{V_{wz}}{\Delta V}} \quad [32]$$

in which the z subscript represents initial values, and

$$b = \gamma_s/\gamma_w, \text{ and} \\ \Delta V = (q_i - q_o)\Delta t$$

For the special case of ΔV very small compared with V_w , one obtains a different form of solution:

$$T_o = T_i + (T_{oz} - T_i) \exp\left(\frac{-q\Delta t}{V_w + bV_s}\right) \quad [33]$$

Equation [32] or [33] is solved for each computational element in the soil column in which water moves during the time step. The water volume and flux terms are obtained from the water movement computations. the most dramatic heat convection occurs in the influx of large amounts of generally cooler rainwater. In the absence of actual data on rainwater temperature, it is assumed to be equal to the minimum daily temperature for the day of occurrence.

Transport of Solutes through Soil

Opus includes the capability of calculating the transport of partially sorbed chemicals in the flow of unsaturated soil water. One of two kinds of reversible absorption processes may be simulated: (a) adsorption assumed to be characterized by an equilibrium linear isotherm, or (b) non-equilibrium kinetic adsorption, following a linear isotherm. The kinetic transfer assumes that the rate of adsorption or desorption is linearly related to the difference between the current phase ratio and the equilibrium phase ratio.

Equilibrium adsorption means that there is an invariant ration between the solute adsorbed to soil particles (adsorbed phase) and the concentration in solution (the dissolved phase). Adsorbed material is expressed in solid concentration, as kg/kg-soil. Solutes are expressed in liquid concentration, as kg/l. If the material changes phase slowly in response to a change in the liquid concentration, the kinetic model is appropriate. The equilibrium model does not require instantaneous response to maintain equilibrium, but rather the time scale of phase change response must be smaller than the time scale of inflow of solute with a different concentration.

The equilibrium ratio is expressed with the parameter K_d [units of liters/kg]:

$$K_d = \frac{C_a}{C_w} = \frac{\text{adsorbed concentration}}{\text{dissolved concentration}} \quad [34]$$

Since values of K_d for pesticides is generally proportional to soil organic matter, the pesticide K_d values are usually given as parameter called K_{oc} which is multiplied by soil organic carbon weight fraction, f_b , to obtain the K_d :

$$K_d = f_b K_{oc} \quad [35]$$

If this formulation were universally accurate, K_{oc} would depend on only the type of chemical. However, K_{oc} generally varies with soil type and with chemical species, and use of equation [35] does explain much of the variation in adsorption properties of most pesticide chemicals. Data bases are published with suggested values for most commercially available pesticides.

The assumption of kinetic adsorption accepts the concept of the K_d but specifies a rate of transfer between the two phases proportional to the extent to which the ratio differs from the equilibrium ratio:

$$\frac{dC_a}{dt} = v(C_w K_d - C_a) \quad [36]$$

in which v is rate coefficient with units of minutes⁻¹. Comparing equations [36] and [34] one can see that there is no rate of transfer when equation [34] is satisfied.

Transport with Equilibrium Adsorption A definition sketch for the transport of solutes through an arbitrary numerical layer in Opus is given in figure 17. The approach is similar to that of heat in the previous section, where the partial differential equation is reduced to an ordinary differential equation at the layer scale, with complete mixing¹. The finite layer formulation is

$$\frac{d}{dt} C_w (V + c_h K_d M_s) = C_i q_i - C_o q_o \quad [37]$$

in which

- C_w is concentration in solution in layer (kg/l),
- M_s is mass of soil in layer (kg/ha),
- c_h is a conversion factor [0.0001 ha-mm/l],
- C is value of C_w in or out of layer, depending on subscript (i or o),
- q is inflow or outflow, depending on subscript.

With complete mixing assumed, and when q_i and q_o are both positive, $C_o = C_w$, and one term of the equation is eliminated. Expanding the differential on the left, noting that dV/dt is Δq , and grouping terms, equation [37] becomes:

$$\frac{dC_w}{C_i - C_i} = \frac{q_i dt}{V_{wz} + t\Delta q + K_d M_s c_h} \quad [38]$$

This equation also holds for the case of reversal of both inflow and outflow flux, by symmetry. When both flows are into the layer, this equation will not hold, but changes in C_w can be found

¹ Complete mixing need not be assumed. The equations can be reformulated to include a mixing ratio that goes from 0 (all old water is moved forward) to 1 (complete mixing as shown here.)

by simple summation, because the layer in that case is a “sink”. When both flows are out of the layer, it is a “source”, and the concentration remains unchanged over Δt .

Solving equation [38] for nonzero Δq , the change in local solute concentration after a time Δt , beginning at time t_z with $C_w = C_z$ is

$$C_w(\Delta t) = C_i + (C_z - C_i) \left[\frac{V_{wz} + K_d M_s c_h + \Delta V}{V_{wz} + K_d M_s c_h} \right]^{-V_i / \Delta V} \quad [39]$$

in which V_i is the volume of water entering the layer (mm), and ΔV is the change in storage in the layer, mm.

The form of the solution is parallel with that for heat shown in equation [32]. Flow and volume variables are all obtained from the solution of the water flow equations over the same time step. The outflow concentration from any layer may vary with time, according to equation [39]. To simplify concentration calculations the outflow concentration for any layer is converted to the time average for use as input to the adjacent layer into which it flows. While equation [39] may for this purpose be integrated over time, it is more straightforward to obtain this by mass balance as follows:

$$C_m = \frac{C_z (V_z + K_d M_s c_h) - C_{\Delta t} (V_{\Delta t} + K_d M_s c_h)}{q_o \Delta t} \quad [40]$$

in which subscript Δt refers to values at the end of the time interval, and subscript z refers to values at the beginning of the interval, and C_m is the time averaged mean outflow concentration. For the special case of through flow without significant volume change ($q_i \approx q_o$) equation 38 simplifies and the solution for $C_{\Delta t}$ is

$$C(\Delta t) = C_i + (C_z - C_i) \exp \left[\frac{-q \Delta t}{V} + K_d M_s c_h \right] \quad [41]$$

The solution procedure begins at the layer or layers which are “source” layers (outflow only) and proceeds, calculating outflows in either direction until all inflows to “sink” layers are known, and their new concentrations can be calculated.

Transport with Kinetic Adsorption The option to use equation [36] for transport requires a mass balance equation for each of the phases. Figure 17 illustrates the linked systems. for the dissolved phase, one can write, assuming V is linearly increasing or decreasing during Δt :

$$\frac{d}{dt} (C_w V) = -M_s c_h \frac{dC_a}{dt} + q_i C_i - q_o C_o \quad [42]$$

This equation can be solved in tandem with equation [36] for kinetic gain or loss of adsorbed material. The form of the solution varies somewhat with the various conditions of inflow and outflow. Special cases exist at the upper boundary, where evaporative outflow will take no dissolved material and where input may be free of solutes. In general, when the terms of the equation are of equal order, the Runge-Kutta method can be used for a piecewise solution through the time interval of interest. Total time simulated may be as great as one day.

However, when chemicals have a very high value of K_d so that most of the material is in the form of C_a , it is like a buffered system, and the equation can reduce to the form

$$\frac{d}{dt}(C_w V) = c_h M_s v (K_d C_w - C_a) + q_i C_i - q_o C_o \quad [43]$$

Here C_w is written for C_o , which is true for complete layer mixing except when q_o is evaporative outflow. Even for slowly changing C_a , this equation can be superior in stability to a Runge-Kutta solution. The general solution to [43], starting with dissolved C_z at the beginning of interval Δt , is

$$C_w(\Delta t) = C_b + (C_z - C_b) \left[\frac{V_z}{V_z + \Delta q \Delta t} \right]^{b/\Delta q} \quad [44]$$

where $b = q_i - q_o + v M_s c_h K_d$, and C_b is a steady-state concentration defined by

$$C_b = \frac{q_i C_i + v M_s c_h C_a}{b} \quad [45]$$

As Δq becomes very small, the exponent in [44] becomes excessively large. For this case however the solution of [43] reduces to

$$C_w(t) = C_b + (C_z - C_b) \exp\left(\frac{-b\Delta t}{V_z}\right) \quad [46]$$

For either equation [44] or [46], one can obtain the mean outflow concentration for the interval by integrating or using mass balance as was done in obtaining equation [40]. Opus uses one of these two equations when K_d is more than 40, and selects [46] when the exponent ($b/\Delta q$) in equation [44] exceeds 10. In either case, the time steps used follow the solution appropriately, and the small changes in C_a that occur with the large values of K_d are computed stepwise by a mass balance equation. The kinetic option is useful only for values of v smaller than 0.01 min^{-1} , because larger values are, on a dialy basis, practically indistinguishable from the equilibrium case.

Implementation by Computer Simulating the ensemble of many soil computational layers over a time interval requires consideration of one of several possible cases, depending on the direction of flow and phase transfer model. As indicated above, a layer may be (a) a sink, with flow entering both sides; (b) a source, with flow moving away from both sides; (c) a flow-through layer, with some water entering one side and some leaving through the other; (d) a surface “source”, with water leaving at both sides but no solutes leaving at the top; (e) a surface flow-through layer with water and solute coming in from below but only water leaving above; or (f) the reverse of case (e). For each case, equation [37] or [42] will be modified by elimination of terms or with zero coefficients. This resolution of terms is done prior to solution by either equilibrium or kinetic methods. For each case, the solution order is determined in advance, so that inflows from adjacent layers are calculated prior to a flow-through or a sink layer calculation. The kinetic-solution algorithm uses internally determined time subdivisions for the Runge-Kutta method when dC/dt is rapidly changing

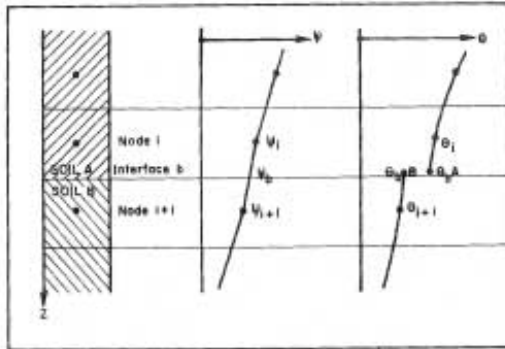


Figure 14. Diagram of changes in Ψ and Θ across the interface of two different soils, and values used at adjacent computational nodes.

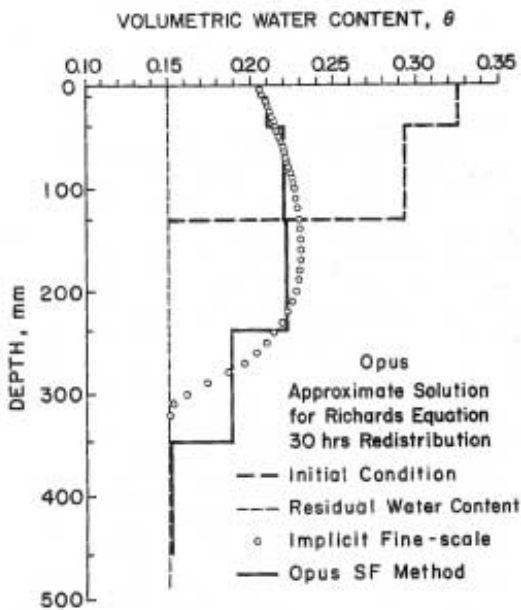


Figure 15. Comparison of the Separable Flux numerical method of Opus (with large depth increments) with a numerical solution of the standard Richards' equation formulation (with very small depth increments). The SF method does a good job of simulating the general distribution of soil water. Use of very large increments with standard numerical methods produces biased estimates of soil-water redistribution.

DRAINTILE SIMULATION

Dynamic balance of saturated zone:

$$V = \int_0^{y_s} \phi h_m dy \approx \phi \bar{h} y_s$$

unsaturated flux = $q(z, t)$

$$\frac{dV}{dt} = \phi y_s \frac{d\bar{h}}{dt} = y_s q(z, t) - q_d(h_m)$$

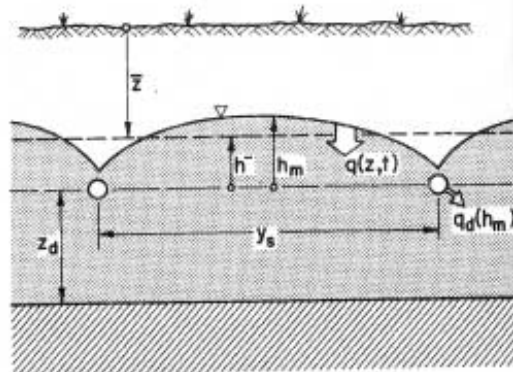


Figure 16. Estimation of drainage for perched or high water table with draintiles. Approximate equations taken from Bouwer and van Schilfhaarde (1963) are used as a lower boundary condition for the unsaturated zone redistribution calculations.

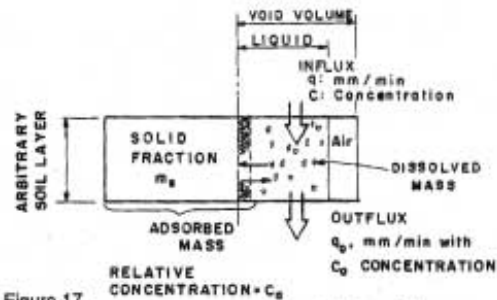


Figure 17. Diagram for model of dissolved/adsorbed chemical movement using the soil increments and interlayer fluxes from the soil water flow model. This figure shows the major terms used in the equations.

5. Surface-water Processes

Much of the pollution from agricultural areas is carried in runoff from precipitation. Surface runoff interacts with the soil and transports dissolved or suspended pollutants off the field or catchment area. Although many of the potential pollutants may be within the soil profile, they are often concentrated near the soil surface. Clearly a useful simulation of the pollution from a field requires an accurate practical simulation of the movement of water on the field surface as well as within the soil.

The difficulty in simulating surface-water processes is not so much in our knowledge of the water movement mechanisms, but rather in having data appropriate to our ability to represent the mathematics of these processes. Specifically, even when data on surface topography and soil are abundant, knowledge of only daily or storm rainfall totals is inadequate for accurate simulation of either infiltration rates or runoff rates. A storm of a given depth may produce large amounts of runoff for high intensities, but produce no runoff if the same depth of rain comes at very low intensity.

Nevertheless, it is most often the case that situations in which simulation is a useful tool do not provide the modeler with the rainfall intensity data that are necessary for using infiltration methods. For this reason, Opus allows the user to choose a surface-hydrology method that is appropriate to lumped daily rainfall data. In addition, since processes of surface-water transport are so dependent on surface-water flow information, the daily hydrology option also uses a lumped method for estimating erosion and sediment production on the catchment. The user's choice of hydrologic option will depend on both the type of data available and the particular objectives of the model user.

Because of the limited information contained in daily rain depth records, and also the lumped nature of the resulting runoff estimation methodology, the information on field topology (Chapter 2) finds only limited use in the daily hydrology option. nevertheless, advantage is taken of all information from the field topology that can be used to improve the accuracy of daily runoff prediction. This improvement includes a refined estimate of the relative time of concentration, which is used to estimate the peak runoff rate.

Simulation of Runoff from Daily Rainfall Data

The minimum hydrologic information needed by Opus from a precipitation event is the amount and the peak rate of runoff. Given only daily total rainfall, these values must be estimated with conceptual or empirical methods based on hydrologic experience. The methods used in the EPIC model (Williams *et al.* 1984) for estimation of runoff amount and peak rate from daily rainfall are used here with minor modification. The SCS Curve Number runoff estimation method is used with some modifications. The basic method is fully explained in the SCS Hydrology Handbook (USDA SCS, 1972). Briefly, runoff amount (Q) is related conceptually to precipitation depth (P), a soil water storage parameter (s_w), and an initial abstraction (I_a) as follows:

$$Q = \frac{(P - I_a)^2}{P + s_w - I_a} \quad [47]$$

$$I_a = 0.2s_w \quad [48]$$

$$s_w = 254 \left(\frac{100}{CN} - 1 \right) \quad [49]$$

The method gets its name from the curve number parameter, CN, defined in Eq. [49]. As indicated, CN may vary between 1 and 100. P, Q, I_a , and s_w are here expressed in millimeters.

Equation [47] was originally described (USDA SCS, 1972) as estimating storm runoff amounts rather than daily amounts. Nevertheless, it is equally applicable to estimate total runoff from rainfall lumped over longer periods. The CN was conceived as a soil parameter with a mean value for mean soil conditions. A method is specified to modify the CN for wet or dry initial soil conditions. The EPIC modifications used in the daily option of Opus relate the value of s_w and thus the CN to current soil water conditions (Williams *et al.* 1984). Opus also uses the method of EPIC to estimate peak runoff rate for each event, based on estimated time of concentration, monthly distribution of mean rainfall intensities, and the ratio of maximum 30-minute and 24-hour rainfall depths for the location of interest (Williams *et al.* 1984).

Unlike EPIC, Opus provides (and the author encourages the use of) an option to use the CN runoff prediction as an expected value rather than a prediction. Thus for long-term simulation sequences, individual runoff amounts are randomly selected from a rational distribution about the CN prediction as a mean. The physical limits of the runoff/rainfall ratio are 0 and 1, and a two-parameter beta distribution with these limits is used. Figure 18 illustrates the shape of the curve described by equation [47] and also the typical scatter of runoff data from two catchments with rather long records (Montgomery 1980). Some scatter of the CN-estimated runoff occurs because the CN changes with initial estimated soil water content. But as figure 19 shows, this scatter is a minor amount compared to scatter in recorded data. Such scatter is to be expected for many reasons, but especially because of the variation in storm intensities. This variation is important information not measured by lumped daily or storm rainfall totals. Figure 20 illustrates the beta function distribution of runoff used in Opus for several given runoff/rainfall ratios.

Simulation of Runoff from Rainfall Intensity Data

Given adequate rainfall intensity data, and entirely different simulation method is available in Opus. A deterministic, distributed simulation of the dynamics of infiltration and surface water flow is done when breakpoint or pluviograph data are provided.

Infiltration Soil water flow dynamics are described by a combination of Darcy's law and an expression for mass conservation. similarly for infiltration, analytic expressions are derived from an equation which combines Darcy's law with and expression for continuity across the soil surface. Assuming that the initial water content θ_i is relatively uniform with an infiltration rate $f(t)$, the basic equation (Smith 1981b)(not derived here) is

$$I = \int_{\theta_i}^{\theta_s} (\theta - \theta_i) \frac{D(\theta)}{f - K_s} d\theta \quad [50]$$

in which

D is diffusivity, defined as $K d\psi/d\theta$ [mm^2/min],

I is depth of infiltration from start of rainfall [mm],
 f is rate of infiltration [mm/min].

and other symbols are as define in chapter 4.

Two types of infiltration condition may be encountered at the soil surface. The first is an imposed ponding conditions, such as with flood irrigation. This effectively imposes a fixed soil-water head at the surface, and equation [50] describes infiltration rate, f for all values of $I > 0$ under these conditions. The other surface condition is the common rainfall or flux boundary condition. For this case, I increases at first due to rainfall, such that

$$I = \int_0^t r(t)dt \quad [51]$$

until the surface becomes saturated, and the boundary condition changes to a fixed head of 0. Consequently, beyond that time the infiltration capacity is controlled by the conditions near the soil surface. This point of control change is called the time of ponding, t_p , after which f is described by equation [50]. These two relations are illustrated in figure 21. At $t \geq t_p$, equation [50] describes the relation between rainfall rate, initial water content (θ_i), and ponding depth, I_p .

An analytic function may be obtained from equation [50] by making some assumptions of the functional form of D that allow integration (Parlange and Smith 1976). The function used in Opus is that developed by Smith and Parlange (1978) which assumes exponential behavior of K near θ_s so that D is approximately proportional to $dK/d\theta$, and equation [50] can be integrated to obtain

$$I = G(\theta_i) \ln \left(\frac{f}{f - K_s} \right) \quad [52]$$

which can be inverted to find $f(I)$:

$$f = K_s \frac{\exp(I/G)}{\exp(I/G) - 1} \quad [53]$$

in which G is a coefficient which depends on initial conditions and on the integral or mean capillary properties of the soil. For most initial water contents, G can be represented as

$$G(\theta_i) = H_c (\theta_s - \theta_i) \quad [54]$$

in which H_c is an effective capillary drive or capillary scale parameter. It is relatively independent of initial conditions, and can be obtained from experiments or from knowledge of the soil conductivity characteristic:

$$H_c = \frac{1}{K_s} \int_{-\infty}^0 K(\psi) d\psi \quad [55]$$

The value of H_c is calculated from the hydraulic characteristic parameters furnished for the surface soil, or those estimated by the regression, if needed. Equations [52] and [53] are

universal insofar as they apply to either predict the time of ponding (by solving equation [52] using $f=r$ until it is satisfied), simulate the pattern of f after ponding, or simulate the pattern of f for suddenly flooded soil under irrigation. Other closely related such expressions [e.g. Green and Ampt] can also be obtained from equation [50] by making alternative assumptions.

During model calculations, computations step forward in time, and an explicit time function for f (or more precisely, ΔI , is useful. For this purpose, equation [53] is first integrated with f expressed as dI/dt , to obtain:

$$K_s t = I + G[\exp(-I/G) - 1] \quad [56]$$

which is used with a Taylor expansion and the finite differential expression that

$$f \rightarrow \frac{[I(t + \Delta t) - I(t)]}{\Delta t}$$

to obtain

$$\Delta I = G \sqrt{B^2 - \frac{2K_s \Delta t}{G \exp(I/G)}} - B \quad [57]$$

in which B is $\exp(I/G)$. This expression is convenient for advancing in small time steps during model simulation, with maximum errors on the order 1 percent. Mean time-step infiltration rate f is taken as $\Delta I/\Delta t$. Note that this expression is asymptotically correct at both small and large values of I . At small I , f is proportional to $1/I$, or I is proportional to $t^{1/2}$, and as I approaches ∞ , f approaches K_s asymptotically.

Treating storm and Soil Complications To use this theory in field runoff simulation, one should be able to account for a variety of complexities presented in real conditions. This section describes how some common complicating factors are treated in Opus. It should be kept in mind that allowance for deterministic complications by the methods outlined here can improve simulation accuracy only to a certain degree. The major ground between mathematical simulation and natural systems performance is occupied by complexities of spatial and temporal variations that are always found in natural catchments. Treatment of such variability is within our capability, but the collection of information on the variability is usually very uneconomic. In some cases, the variability of nature coupled with the sensitivity and nonlinearity of hydrologic processes can cause the deterministic system response to be dominated or obfuscated by the variability. This possibility should not be used, however, to dismiss the utility of physically sound models.

Rainfall Hiatus When rainfall ceases for a period within a storm, runoff will not be generated, and the infiltration capacity will be somewhat recovered. Any runoff water traversing the surface will remain subject to infiltration. The desaturation of the surface soil when there is no surface water proceeds according to the unsaturated soil water equations. At large times after the beginning of such a drainage period, given that r remains below K_s , the surface water content (θ_o) approaches the gravity drainage value, which is (from equation [4]):

$$\theta_o = \theta_r + (\theta_s - \theta_r) \left(\frac{r}{K_s} \right)^{-1/\varepsilon} \quad [58]$$

A rainfall hiatus in Opus, as distinguished from separately treated storms, is less than 180 minutes. For such short periods, a value of θ_o is calculated, and the surface saturation is approached asymptotically with a half life of 30 minutes. The asymptotical approach is made to be a function of the proportion of surface still covered with water, the amount of rainfall already infiltrated (I), and the value of K_s for the soil, as follows (Woolhiser *et al.* 1990):

$$\theta^j = \theta^{j-1} + [\theta_o - \theta^{j-1}] \left[1 - \exp\left(\frac{-c_r}{\Delta t}\right) \right] \quad [59]$$

in which j is the time step index, and

$$\begin{aligned} \Delta t & \text{ is } t^j - t^{j-1}, \\ c_r & \text{ is a rate parameter: } c_r = K_s/(I + 0.1) \end{aligned} \quad [60]$$

This is a conceptual relation but is similar to one that has proved successful in simulating data from Walnut Gulch experimental watershed. It provides for redistribution to proceed more slowly for large I and for less permeable soils (low K_s).

Infiltration through a Surface Crust Layer_ Another important complication on catchments is vertical anisotropy in the soil profile. Opus treats a general three-layer case for infiltration dynamics. The surface soil is assumed to lie above a subsoil layer, which may be assigned properties by the model user to represent a plowpan condition, for example. The lower soil is may be either less than or equal to the surface soil in hydraulic conductivity, for purposes of infiltration modeling. In addition, a thin surface “crust” layer may be formed on a soil following disturbance such as cultivation. The crust formation is a function of the accumulated impact energy of subsequent rainfall. The following method of simulating the crust and its effect is not theoretically complete, but it does provide for reasonable modification of infiltration rates in response to management changes affecting the surface soil.

The crust layer, when formed, is assumed to change the upper layer of computation, which is 10 mm thick. Although this is certainly not accurate for all cases and all soils, it should be noted that crust thickness and crust hydraulic conductivity play interchangeable roles in infiltration dynamics (Smith 1990).

The Opus infiltration model assumes that the saturated hydraulic conductivity of the crust, K_{sc} , is equal to or less than the underlying soil, K_{s1} . The converse case is both unusual and relatively ineffective in altering infiltration rates. When the ratio of r to K_{sc} is large, ponding could theoretically occur with wetting not yet extending beyond the crust depth, $I < I_c$. I_c is the value of I to just fill the crust layer. In such a case, calculation of t_p is straightforward.

Ponding is more likely to occur after the wetting front has passed through the crust layer, $I > I_c$. For this case, the crust and the underlying soil both play important role in the net infiltration dynamics (Smith 1983b, 1990). The final infiltration rate is altered, and is lower than that of the underlying soil but greater than that of the crust. It is found by analysis of steady unsaturated flow across the two layers (Smith 1990).

The vertical distribution of soil water potential in this case will be something as shown in figure 22. At longer times, the gradient in the underlying soil becomes small, and the value of K_1 becomes closely uniform, and a steady gradient is approached in the crust. By matching fluxes

fluxes into and out of the boundary, and matching heads for both soils at the boundary (ψ_b), one can write:

$$K_c(\psi_b) \left[1 - \frac{d\psi}{dz} \right] = K_1(\psi_b) \quad [61]$$

This equation may be integrated through the crust depth, assuming the right side is a constant at large times:

$$z_c = \int_0^{\psi_b} \frac{d\psi}{\frac{K_1(\psi_b)}{K_c(\psi)} - 1} \quad [62]$$

The function $K(\psi)$ is described in equations (2) and (4), and $K_1(\psi_b)$ is a single value satisfying this function for ψ_b . Equation [62] is integrated by trial or iteration to find ψ_b and $K_1(\psi_b) = K_{se}$, which is the asymptotic infiltration rate for the crusted case.

In most cases, the best single value of G to use when the wetting front has passed through the crust into the subsoil is that of the subsoil, G_2 . This approximation comes from a study of infiltration under various conditions with various crust properties. At short times, equation [55] is accurately approximated by the expression

$$f = \frac{GK_s}{I} \quad [63]$$

When the subsoil has a higher K_s and the value of $K_{se}G_1$ is lower than K_sG , the value of G_1 should be used for $I > I_c$. When $K_{se}G_1$ is larger than K_sG , it is more accurate to use a weighted value of G for $I > I_c$. To estimate the weighted value, a G' is found such that $G'K_{se} = GK_s$. Then as I increases beyond I_c , G for use in estimating $f(I)$ is found as a weighted average of G' and G_1 (Smith 1990) as follows:

$$G_e = \frac{I - I_c}{I} G' + \frac{I_c}{I} G_1 \quad [64]$$

and G_e is used along with K_{se} in the infiltration model. Although this procedure may seem complex, it is handled automatically in Opus, and provides a smooth simulation of the changes in infiltration rates. One case simulation is illustrated in Figure 23.

Crust Development The formation of surface crusts on a wide variety of disturbed bare soil is well known but the mechanics of transient surface-crust layer development in agricultural conditions are poorly understood. There is yet no reliable prediction of crust formation based on measured soil characteristics. Crust development apparently depends on such things as particle size distribution, clay and organic matter content, exposure to rainfall energy, and distribution of raindrop sizes (Chevalier 1984). It is a subject needing much more investigation. It is known that the hydraulic conductivity of rainfall-induced crusts is commonly an order of magnitude less than that of the parent soil, with some noted exceptions (Chevalier 1984). Further, in the absence of soil cohesion, the crust development is probably limited to simple increases in bulk density due to packing.

The hypotheses used in Opus to estimate K_s reduction during crust formation is illustrated in Figure 24. The upper graph represents the hypothesis for the maximum reduction that can be achieved in a crust, and shows that crust potential is assumed to be highest for intermediate clay contents. The lower graph illustrates Opus' hypothesis of the rate of crust formation as a function of cumulated rainfall energy, measured by the EI of the USLE relationship. The storm effective EI that is used to estimate crust reduction of K_s is directly reduced by the ratio of cover (mulch and plants). Opus uses the EPIC regression method to estimate EI when daily rainfall data are used, and finds an approximate storm EI using

$$EI = 10 r^2$$

when breakpoint rainfall rates, r , are given in mm/min.

Crusts are assumed to be destroyed by cultivation operations that disturb the soil to any depth. Because some operations will not completely destroy an existing crust, the specified efficiency of cultivation ($0 < e_c < 1$.) determines the starting state, EI_o , as follows:

$$EI_o = -400\sqrt{e_c} \quad [65]$$

In part, this conceptually represents the effect that cultivation has on opening the soil, which goes beyond merely destroying a previously formed crust. Thus the soil hydraulic conductivity is briefly enhanced by a negative EI as a leftward extension of the lower graph in figure 24. Succeeding rains quickly increase the summed EI into the positive region (e.g., clod dissolution).

Dynamics of Surface Water

When the infiltration simulation model begins to produce rainfall excess, water begins to move over the surface (excepting the case of flat surface furrow storage) along the described topography. Because Opus is limited to areas containing insignificant large scale variations of soil, all parts of the catchment are assumed to begin to produce runoff at the same time. The tracking of spatial and temporal variations in surface-water flow conditions is crucial in simulating not only the discharge at the catchment outlet, but also the transport processes within the catchment that produce the pollutant load of dissolved and suspended material at the outlet.

The de Saint-Venant equations for surface water flow have proven to be a reasonably accurate and efficient description of the dynamics of catchment runoff. Two alternate well-known approximations are used in Opus to solve these equations. The kinematic wave approximation assumes that an equation of material balance and a rating equation are sufficient for all but very flat slopes. For very low slopes, a diffusive wave equation is used, slightly more complicated than the kinematic wave equation, but amenable to rapid solution. The rating equation describes a consistent relation between discharge and depth or area for a given section geometry. The Manning uniform flow formula is such a rating, and is the one used in Opus. It relates flow velocity to hydraulic radius. Hydraulic radius, R , is defined as the flow cross-sectional area divided by the wetted perimeter. Material balance expressed in differential form is

$$\frac{\partial a}{\partial t} + \frac{\partial q}{\partial x} = (r - f)w \quad [66]$$

in which

- a is cross-sectional area of flow (m²),
- x is distance from beginning of runoff path (m),
- q is local discharge (m³/m/min),
- t is time in minutes,
- w is local flow width (m),
- r is current rainfall rate (m/min), and
- f is current infiltration rate (m/min).

The Manning equation for normal flow can be expressed (in units here used) as

$$q = 60 \frac{\sqrt{S}}{n} \rho R^b \quad [67]$$

in which

- S(x) is local water energy slope,
- n is manning roughness coefficient,
- ρ is wetted perimeter, (m),
- R is hydraulic radius (m),
- b is hydraulic exponent, = 5/3 for the manning relation.

Equations [66] and [67] are also tied together by the fact that $a = \rho R$. Thus, equation [66] may be written in finite difference form for solution as follows:

$$\begin{aligned} & [\rho R]_i^{j+1} - [\rho R]_i^j + \frac{\Delta t}{\Delta x} \omega [q_i - q_{i-1}]^{j+1} + (1 - \omega) [q_i - q_{i-1}]^j \\ & - w \left\{ \omega [r - f]^j + (1 - \omega) [r - f]^j \right\} = F(R_i) = 0 \end{aligned} \quad [68]$$

in which i and j refer to sequential distance and time increments, respectively, of size Δx and Δt. When the flow section geometry is given, the relation between a, R, and ρ can be obtained, since $q_i = q(R_i)$. Thus equation [68] can be solved for R_i^{j+1} by iteratively making the objective function $F(R_i) = 0$. The Newton-Raphson method for sets of equations is used, and the matrix equation has the form

$$\mathbf{J}(3,n) \delta(\vec{R}) = F(\vec{R}) \quad [69]$$

where $\mathbf{J}(3,n)$ is the tridiagonal jacobian coefficient matrix, containing terms $\partial F/\partial R$,
 $\delta(\vec{R})$ is the vector of estimated corrections to \vec{R} , and
 $F(\vec{R})$ is the vector of residuals as in equation [68].

The upstream and downstream boundary conditions depend on the flow type as discussed below.

Kinematic Wave Flow Morris and Woolhiser (1980) demonstrated a criterion on the basis of which one can properly assume kinematic flow for larger slopes or for shallower depths. This criterion may be called the *kinematic wave number*, k_o , which is defined as follows:

$$k_o = S_o L / h_o \quad [70]$$

in which S_o is the bed slope, L is the flow length (m), and h_o is the normal flow depth (m). When k_o is greater than about 5 for low Froude numbers, the kinematic wave approximation is appropriate. That is, the slope term in equation [67] can be assumed to be the bed slope. For rainfall on a kinematic slope with an upstream divide, the upper boundary condition is simply that $q = 0$, or $R(0) = 0$. For cases where a small channel has an upstream input q_o , the upstream boundary can be specified as $R(0) = R(q_o)$, or the normal flow depth for discharge q_o . This requires an algorithm to invert the rating equation $q(R)$ for a given flow geometry. The kinematic flow assumption requires no downstream boundary condition. The formulation equation [68] for the finite difference solution allows either sequential solution starting at the upstream boundary and working downwards to $i=N$, or a matrix solution for all i at once as in equation [69]

Diffusive Wave Flow When k_o is smaller than 5, the kinematic wave approximation is generally inadequate, and the energyslope may then be expressed as

$$S = S_o(x) - \frac{dh}{dx} \quad [71]$$

Use of equation [71] in equation [68] makes the formulation more complicated and nonlinear, so that sequential solution is not possible as in the kinematic case. In Opus, the depth h in equation [71] is approximated by R . In addition, a relaxation coefficient is required for iteration. This means that stability of convergence is aided, for the $(k+1)^{th}$ iteration by estimating

$$R_{k+1} = \beta(\delta R_{k+1}) + R_k$$

in which δR is the correction to R found from equation [69] and k is the iteration number. The upstream boundary condition for diffusive wave flow is, with no inflow, $S(0) = 0$, or $dh/dx(x=0) = -S_o$. As for kinematic wave flow, an upstream boundary with inflow assumes a normal flow depth. The usual downstream boundary condition for diffusive wave flow is a critical depth condition, which is consistent with a free overfall. While this is not always the case, it is not a severe assumption, and allows convenient computation of a flow-depth relation. The alternative is a more complex backwater calculation.

Estimation of Hydraulic Roughness With the purpose of Opus to simulate hydrologic behavior under complex management changes, it is not realistic to use a fixed value of n , and so some method must be devised to estimate the changes of n with management operations. The user of Opus may specify a value of Manning n to represent roughness, which is used until a surface altering management operation takes place. For natural untilled catchments, this value will apply throughout the simulation.

When the field is tilled, and empirical estimate is made of the resultant roughness, n . It is assumed to be the sum of four factors: a bare soil value for smooth, clean soil surface; a roughness caused by surface residue; a form roughness caused by clods and irregularities caused by plowing; and for unfurrowed surfaces, the roughness effect of plants and their stems. For many cohesive soils, the actual form roughness from plowing can vary considerably, depending on the soil wetness at plowing. The relationship is unquantified and needs further research, and Opus does not treat it yet.

The value of n for bare smooth soil is assumed to be 0.02. Form roughness, f_f , varies with the type of operation and equipment. A table of values as a guideline is given in the User Manual (Vol. 2), taken partly from work done for EPIC (Williams *et al.* 1984). Values range from 6 to 50, representing mean height in mm of microroughness forms. The resulting hydraulic roughness effect, in terms of a partial Manning n_f is estimated (G.R. Foster, personal communication) as:

$$n_f = 0.00087f_f^{1.25} \quad [72]$$

The roughness resulting from surface residue is estimated following the work of Foster *et al.* (1982). It is a function of effective residue weight (m_{res} kg/ha) and a coefficient (c_{res}) that changes between furrowed and unfurrowed flows. The effective mulch cover is first estimated as

$$F_m = 1 - \exp\left(\frac{-m_{res}}{4428}\right) \quad [73]$$

The partial residue roughness, n_{res} , is then estimated according to the data from Foster *et al.* (1982) by:

$$n_{res} = \left[1 + \left(\frac{c_{res}}{m_{res}}\right)^2\right]^{-0.61} \quad [74]$$

The value of c_{res} is 10.67 for furrowed surfaces and 3.43 for unfurrowed surfaces, according to Foster *et al.* Finally, the weighted sum of form and mulch factors becomes a partial n value represented by

$$n_{rf} = F_m n_{res} + (1 - F_m) n_f \quad [75]$$

When the flow encounters vegetation in its path, particularly for unfurrowed flow, the estimation is made on the basis of plant stem density. This is taken as a function of plant mass per unit surface area. The estimating equation is

$$n = \left[n_{rf}^{3/2} + n_b^{3/2}\right]^{2/3} + 3.6 \times 10^{-6} \frac{M_{lv}}{y_p} \quad [76]$$

in which M_{lv} is mass of plant above ground in kg/ha, and y_p is height of plant in m.

Flow Geometry Relations The flow section geometry for which equation [68] can be applied is quite arbitrary, including a flat surface; furrows; and trapezoidal, triangular, or rectangular channels. When a furrow or channel is treated, often a relatively flat bottom is formed by transport and deposition of sediment. This surface can have a very different roughness than do the sides of the section. In such a case, the local net value of Manning roughness (\bar{n}) may be treated as the weighted sum of the values of n of each part of the wetted perimeter, as follows:

$$\bar{n} = \left[\frac{(\rho_b n_b^2 + \rho_z n_z^2)}{\rho} \right]^{1/2} \quad [77]$$

in which subscript b refers to the bottom section and subscript z refers to the side slopes.

Time Steps Hydraulic conditions on the catchment are checked at each time step, and time intervals are reduced if velocities are large enough with respect to x increment size to cause instabilities. If a reduced time step is indicated, it is applied at the next calculation time. The largest time steps allowed are those read from the rainfall intensity record. Time steps those for the infiltration calculations, described above are the same as for surface water routing.

Irrigation Flows The numerical scheme described above is in principle applicable to estimating the advance of water down a furrow during border irrigation, or the runoff (if any) from sprinkler irrigation. Sprinkler irrigation applications are treated simply as uniform rainfall. For border irrigation, the limits of practicality do not allow Opus to divide long furrows into enough distance increments to produce a precise simulation of furrow advance, but Opus provides a reasonable approximation. The principal additional feature required for irrigation-advance simulation is the proper calculation of the spatial variation of infiltration rate, which depends on the time of initial wetting at any point along the furrow. Thus, infiltration rate f and depth I are separately calculated for each increment node (x_i) along the furrow. Net infiltration for water-balance calculations is obtained by summing over all locations along the furrow.

Erosion and Transport of Sediment

The methods used by Opus to estimate the sediment production resulting from rain on a catchment correspond in approach to the methods available for estimating runoff. The sediment option accompanying the daily runoff method is necessarily a lumped-parameter expression that corresponds in sophistication to the SCS Curve Number method. The corresponding option associated with breakpoint rainfall is a spatially distributed treatment of sediment transport similar to KINEROS (Smith 1981a). The method has been expanded to allow simulation of sediment with up to five representative particle size classes.

For all cases, information on the rate of erosion (or deposition) as a function of soil, surface, cover, and local hydraulic conditions is crucial for accurate estimation of sediment transport. Opus makes use of information on the local conditions that is available from other parts of the model, including plant and mulch cover, and soil-surface conditions.

Sediment Production for Daily Simulation The daily amount of sediment that is produced by a day with runoff is estimated with a variation of the well-known USLE (Wischmeier and Smith 1978), which is MUSLE (Williams 1975). USLE is a lumped-parameter method of estimating net erosion by use of a log-regression expression involving a parameter estimate of each of several major erosion factors, as follows:

$$Q_s = R_u K_u L_u S_u \phi P_u \quad [78]$$

in which

Q_s	is net storm or daily soil loss [kg/m ²],
R_u	is storm or daily erosivity [Newtons/hr],
K_u	is soil erodibility factor [kg-hr/Newton/m ²],

- L_u is slope-length factor,
- S_u is slope steepness factor,
- ϕ is a coefficient for cover and management, and
- P_u is a factor for effects of supporting management practices.

Use of the USLE and detailed discussion of the coefficients and their values is provided in the USDA handbook on the subject (Wischmeier and Smith, 1978). In MUSLE, R_u is modified from the original USLE to account for both rainfall and runoff erosivities. The estimating equation is

$$R_u = 90.5 (Q \cdot q_p)^{0.56} \quad [79]$$

in which Q is the runoff in m^3 and q_p is the peak runoff rate in m^3/s . Clearly this is a lumped approximation, but the method has been tested and has a complexity appropriate to the daily runoff estimation method. The effects of impoundments such as tile outlet terraces or holding ponds are simulated by modifications to the parameter P_u .

Distributed Erosion and Sediment Transport When rainfall rate patterns are used (option 2) the runoff calculations provide spatial and temporal distributions of hydraulic variables and allow distributed estimation of sediment transport dynamics. The general governing transport equation (Bennett 1974) for a particle size class k can be written as:

$$\frac{\partial}{\partial t}(aC_{sk}) + \frac{\partial}{\partial X}(qC_{sk}) - wd(x, t)_k = q_s(x, t)_k \quad [80]$$

- in which
- C_s is sediment concentration,
 - a is cross-sectional area of flow [m^2],
 - q is water discharge [m^3/min],
 - w is flow width, m ,
 - d is rate of erosion or deposition at the bed, [$m^3/m^2/min$], and
 - q_s is local input of sediment (if any), [$m^3/m/min$].

This equation may be applied and solved through time and space for each particle size class k , given information on the hydraulic conditions in time and space. It is solved numerically in Opus, in conjunction with the solution for runoff water. Given the change in these values over a time step, the concentrations may be solved directly.

Surface Detachment and Transport Capacity Whether the surface is furrowed or unfurrowed, flow can be thought of as both “sheet” (uniformly distributed) or rill flow. Erosion for both flow types is caused by the dislodging of soil particles by raindrops and by the shear force of water flowing over the soil. For rainfall detachment, d_i , Foster (1982) proposed an equation based on existing experimental data, as follows:

$$d_i = 0.0138 k_u r_e^2 [2.96S_i^{0.79} + 0.56]\phi_i \quad [81]$$

- in which
- r_e is effective rainfall intensity in mm/hr ,
 - S_i is the sine of the surface slope angle, and
 - ϕ_i is the interrill soil/crop coefficient as follows:

$$\phi_i = \phi_u (1 - F_s) \exp \left[-0.21 \left(\frac{h_c}{h_b} - 1 \right)^{1.18} \right] \quad [82]$$

where

- F_s is fractional total plant and mulch soil cover,
- h_c is water flow depth for given conditions, m,
- h_b is water flow depth for bare soil, m,
- ϕ_u is the (USLE) surface soil residue factor, defined as $\phi_u = B_s(c_a + c_b t_m) \exp(-120 f_{rz})$
- B_s is a soil consolidation factor
- c_a and c_b are coefficients,
- t_m is time since last tillage, and
- f_{rz} is residue concentration in surface soil ($\text{kg/m}^2/\text{mm}$)

Foster's concepts grew out of attempts to quantify USLE factors, to some extent, and the ϕ factors are related in concept to those of the USLE, insofar as they represent effects of management on the erosion process. The coefficients are discussed in Foster *et al.* (1983).

The erosion or deposition of particle size class k for distributed surface flow is assumed to obey a linear deficit relationship, derived from basic principles, based on the transport capacity of the flowing water, C_{mxk} as follows:

$$d_{ek} = b_k v_s (C_{mxk} - C_k) \quad [83]$$

in which v_s is settling velocity, and b_k is a coefficient. For rill flow, Foster *et al.* (1983) proposed a similar relation with different rate coefficient

$$d_{rk} = \left(\frac{d_{pr}}{g_c} \right) [g_c - g_s]_k \quad [84]$$

- in which
- d_r is actual local rill detachment rate [$\text{kg/m}^2/\text{min}$],
 - d_{pr} is potential rill detachment rate [$\text{kg/m}^2/\text{min}$],
 - g_c is transport capacity for particle class k [$\text{kg/m}^2/\text{min}$],
 - g_s is current transport rate for class k [$\text{kg/m}^2/\text{min}$]

For this method, Foster *et al.* proposed both d_{pr} and g_c to be related to local hydraulic shear:

$$d_{pr} = b_D \tau_s^{3/2} \quad [85]$$

$$g_c = b_T \tau_s^{3/2} \quad [86]$$

in which b_D and b_T are related to erosion coefficients and clay content, f_c , as follows:

$$b_D = 139 k_u \phi_u \phi_r \quad [87]$$

$$b_T = 188 - 468 f_c + 907 f_c^2 ; \quad f_c \leq 0.22 \quad [88]$$

$$b_T = 130 ; \quad f_c > 0.22$$

in which ϕ_r is $\exp[-1.8M_m]$ and M_m is mulch cover density in kg/m^2 .

with the shear terms in equations [85] and [86] dividing out in equation [84], this term becomes a constant related to factors ϕ and clay content. Thus it is very similar to equation [83] and the

similar erosion equation used in KINEROS (Woolhiser *et al.* 1990) except for the determination of the rate coefficients.

Potential transport capacity is found in the form of the equilibrium concentration, using the relation of Englund and Hansen (1967):

$$C_{\text{smx}} = \frac{0.05 S u u_*^3}{g^2 h y_d (\rho_s - 1)^2} \quad [90]$$

in which

u	is flow velocity, [m/min],
u_*	is shear velocity [m/min],
y_d	is mean particle diameter [m],
ρ_s	is particle specific gravity,
g	is acceleration of gravity [m/min ²],
h	is flow depth [m], and
C_{smx}	is transport capacity concentration for given conditions.

This relation is chosen because it has been shown to be as robust as any for shallow flows and high slopes, which may often be encountered (Alonso *et al.* 1981). It has been discussed thoroughly elsewhere (Alonso 1978),

Concentrated Flow Erosion and Sediment Transport Here we refer to all channels on the catchment larger than rills. Even in catchments of relatively simple geometry, distributed surface flows soon become concentrated into rivulets or small channels. On managed areas these channel may be the furrows themselves, or they may be formed when flows in furrows find a local swale and form a cross-furrow flow. These cases often result in *ephemeral gullies* in areas where erosion potential is high. They are ephemeral in cultivated lands because they are obliterated by mechanical cultivation. Conversely, these swales may be places for upland eroded material to deposit. Foster *et al.* (1983) suggested that erosion rates in small channels are best modeled by a relation based on the hydraulic bed shear and including consideration of a critical or threshold value, as follows:

$$D_f = c_f (1.35 \tau_s - \tau_c) \quad [91]$$

in which

D_f	is the local concentrated flow detachment rate [kg/m ² /min],
c_f	is a coefficient,
τ_s	is hydraulic shear on the wetted perimeter [Newtons/m ²], and
τ_{cr}	is critical shear, above which erosion occurs [N/m ²].

This value is considered a potential detachment rate and is used in equation [84] along with a transport capacity for distributed flow to determine actual local erosion (or deposition) rate. The value of c_f is suggested by Foster *et al.* (1980b) to be estimable as proportional to USLE erodibility k_u ; in Opus, c_f is taken to be $0.246 * k_u$ [metric units].

Erosion and Deposition with Mixed Particle Sizes The transport of sediment particles is possible because of the dissipation of hydraulic energy from the flowing water in which they are suspended. When the soil consists of a mixture of particle sizes (and densities), with different settling velocities, the particle sizes will have different transport capacities. Although there are yet no definitive experimentally-based relationships for the apportionment of

transport energy among particle sizes of a mixture, some reasonable assumptions can make possible a useful model for the process. Opus uses up to five particle size classes to represent a basic distribution of particle sizes and densities. The methods of Foster *et al.* (1985), for estimating the distribution of these classes in the absence of specific analysis, are available as a default in Opus.

In the distribution of transport capacity among particles of a sediment mixture, three general cases can be identified. In the first case, the transport capacity of the flow may exceed the current sediment load for all particle sizes. Here it is reasonable to assume that erosion will act on all particles of the soil, and the rates of erosion will be proportional to the relative fraction of the particle size class in the surface soil.

In the second possible case, the transport capacity may be inadequate to move any of the soil particle size classes, and deposition of any particles in the flow will occur at the theoretical deposition rate, which is the concentration times the settling velocity, $C_{sk}V_{sk}$.

In the third case, conceptual assumptions may be required, and present theory is incomplete. Here the transport capacity may be greater than the current concentration of the smaller or lighter particles, but be less than that of the heavier or larger particles. The model must distribute the hydraulic energy among the particle sizes that make up the total sediment load. In Opus, the limited transport capacity is assumed to be the weighted sum of the transport capacities calculated for each class size. The weightings are assumed to be inversely proportional to the settling velocities of the class size and densities. Thus particle sizes of high transportability will tend to be enriched in the transported mix, compared with those of high fall velocity and low transportability. This would occur not by selective erosion but by preferential deposition. Selective erosion should be self-limiting insofar as the soil surface soon becomes “paved” with particles too large to be detached.

In determining the local conditions for transport of several particle size classes, the total transport capacity of the least transportable class is compared with the total sediment load, and hydraulic detachment is calculated if excess capacity exists. This is distributed according to the particle class composition of the eroding soil. When transport capacity of any class is exceeded by its current concentration, deposition of that class is calculated. This will occur more often for larger and denser classes, and enrichment of fines in catchment outlet runoff will result.

Evolution of Flow Sections with Erosion and Deposition Erosion and deposition often occur alternately during the course of a runoff event at any location, and will alter the geometry of a furrow or a channel. Also, small channels in a catchment will tend to have a geometry that is characteristic of the balance of erosive and depositional forces. With some simplifying assumptions, one can estimate the direction that will be taken in erosive or depositional changes in channel geometry. Opus includes an algorithm to estimate the changes in a furrow or channel section that result from the loss or gain of a certain eroded or deposited volume (expressed as m^3/m)

It is assumed that the channel or furrow cross-section starts as a simple trapezoid or as a triangle formed as the intersection of two slopes, and is reset to such a geometry after any sedimentation by mechanical operations. The width of the bed is assumed to adjust itself until critical shear is exceeded only on the bottom of the section. Changes of section shape are not computed during a runoff event, but are effected after the event when flow means and erosion or deposition totals are known. Erosion of a trapezoidal section can be accompanied by either

narrowing or widening of the bottom section. The same is true in deposition or reduction in section area.

In the model CREAMS, Foster *et al.* (1980a) assumed a simple distribution of the local shear force along the wetted perimeter and developed an algebraic method to predict bottom width based on that assumption. If the flow section is assumed to be rectangular, the hydraulic radius is related to the section factor, SF, as follows:

$$R = c_m [SF]^{3/8} \quad [92]$$

in which $SF = Qn/\sqrt{S_o}$, and
 $c_m =$ a coefficient that depends on section geometry.

The local shear stress is assumed to be distributed along the wetted perimeter, increasing from zero at the water edge to a maximum at the middle of the bottom. To describe this distribution, we define a normalized distance along the wetted perimeter, called y_* . This is obtained by dividing the distance from the water edge by the total wetted perimeter, ρ . The local shear stress distribution is expressed in terms of the mean shear stress and a weighting function B: $\tau(y_*) = \tau_m B$, where

$$\tau_m = \gamma_w S_o R \quad [93]$$

and B is a weighting along y_* such that

$$1.0 = \int_0^{0.5} B(y_*) dy_*$$

If c_m and R in equation [92] are expressed in terms of y_* and combined with equation [93], a combined weighting factor b_c can be obtained as follows:

$$b_c(y_*) = [SF]^{3/8} \left(\frac{\gamma S_o}{\tau_c} \right) \quad [94]$$

The terms on the right can be obtained independently of the section proportions, so the function b_c is found for a rectangular section such that τ at the edge of the bottom is just equal to τ_c . The resulting geometry provides that the width will be

$$w_f = ([SF](1 - 2h))^{3/8} y_*^{-5/8} \quad [95]$$

This provides a means to estimate the width of the bottom when scour or deposition is altering the shape of the section. This method is used in Opus with sloping sides rather than rectangular sections. Figure 25 illustrates how the section is assumed to change. At the end of a runoff event, the amount eroded or deposited at each section has been accumulated and expressed in terms of a cross-sectional area. This is used along with the width found from equations [94] and [95] to solve for the required cross-section. Given a change in section area and a new bottom width, the change in bottom elevation is the single unknown dimension.

Impoundment Storages

One significant management practice that may often be used in controlling pollution from agricultural catchments is the inclusion of an impoundment element in the field. This may take the form of a tile outlet terrace or a series of them, or it may be as simple as a pond at the lower end of the field. Ponds may also be parts of an unmanaged or natural catchment. For experimental catchments, an impoundment may be formed as a backwater to a measuring weir or flume.

The option for daily rainfall and sediment (described above) simulates the effects of a pond on sediment and sediment-associated pollution by modification of the USLE “P” factor (P_u) as specified in the USLE methodology. The USLE handbook describes the appropriate P_u factor changes for pond effects.

Routing Water through a Pond Given the time distribution of inflows of water and sediment to a pond, as simulated by hydrology option 2, the effects of the pond storage on both the hydrograph and the sediment concentration distribution can be analytically estimated.

The pond is described for purposes of simulation either by an equation for the depth-area relationship, or by the slope geometry of the surfaces converging at the pond location. That is, the description of the slope of two planes and the slope of their intersection (presumably a channel to which they contribute), plus the slope of the face of the dam across the channel, can be converted into an equation for the depth-area relation. This geometry forms an inverted pyramid shaped “basin”

Either method produces an equation with three parameters relating pond water surface area (A) to depth (h) as follows:

$$A(h) = A_p + b_p h^{c_p} \quad [96]$$

in which A_p , b_p , and c_p are the descriptor parameters for this pond.

The other information needed to route water and sediment through the pond is the outlet rating relation. This is an equation relating discharge from the pond to its depth (h), and includes a threshold depth below which the discharge is zero. The pond is assumed to seep water into the soil at all depths, using the saturated hydraulic conductivity of the surface soil layer or other user-specified loss rate as the rate of seepage.

The outflow rating may be given either as an explicit relation of the discharge to depth or in the form of an orifice coefficient, which is translated by the program into an explicit relation. The general rating relation for outlet discharge takes the form

$$Q_o = c_o (h - h_z)^{d_q} \quad [97]$$

in which Q_o is outlet discharge [m^3/min],
 h is pond depth [m],
 h_z is the threshold depth for outflow [m], and
 c_o and d_q are parameters.

The routing of runoff through a pond is simply the solution of the differential equation for a linear storage system, as follows:

$$\frac{dV}{dt} = Q_{in} - Q_o \quad [98]$$

in which Q_{in} is pond inflow discharge [m³/min],
 V is the storage in the pond.

and Q_o is defined in Eq. [97]. These equations may be written with h as the dependent variable, finding $V(h)$ by integrating equation [96]:

$$V(h) = \int_0^h A(y)dy = A_p h + \frac{b_p}{c_p + 1} h^{c_p + 1} \quad [99]$$

In Opus, the solution of this system is obtained on successive small time steps (Δt) during which Q_{in} is assumed constant. Using $dV(h) = A(h)dh$, the solution is actually obtained in the form

$$\frac{dh}{dt} = \frac{Q_{in} - Q_o(h)}{A(h)} \quad [100]$$

Pond storage (except for the smallest ponds) will often have a considerable damping effect on the peak discharge from a small catchment. A significant value of h_z indicates that runoff from small flows can be trapped, and pondages in general con trap most sediment carried by all but the larger flows.

Routing of Sediment through a Pond Each particle size class from the sediment transport simulation is routed separately through a pond. A sediment particle entering the pond is assumed to settle at its fall velocity. The general equation for mass balance of the particle class j , with concentration C_j and settling velocity v_{sj} , can be written as

$$\frac{d(C_j V)}{dt} = (C_j Q)_{in} - C_j Q_o(h) - A(h)C_j v_{sj} \quad [101]$$

We solve this equation (as for pond depth) sith small time steps during which Q_o and Q_{in} are assumed locally constant. Noting that dV/dt is $Q_{in} - Q_o$, the general equation for C_j becomes

$$\frac{dC_j}{dt} = \frac{(C_j Q)_{in} - C_j (Q_{in} + A v_{sj})}{V(t)} \quad [102]$$

Equation [102] is solved by a transformation of variables, and the solution takes one of three forms, depending on the relative size of various terms. The forms are:

Form 1: For relatively constant V , or when $Q_{in} \approx Q_o$, the solution for C_j after an interval Δt is

$$C_j = C_{jX} + (C_{jo} - C_{jX}) \exp[-b\Delta t / V] \quad [103]$$

in which C_{jo} is C_j at beginning of interval Δt ,
 b is $Q_{in} + Av_{sj}$, and
 C_{jX} is $C_{ji}Q_{in}/b$.

Form 2: For values of $[b/\Delta Q]$ greater than 10,

$$C_j = C_{jX} + (C_{jo} - C_{jX})V \frac{1 - \exp(b\Delta t/V)}{b\Delta t} \quad [104]$$

Form 3: For values of $[b/\Delta Q]$ less than 10,

$$C_j = C_{jX} + (C_{jo} - C_{jX}) \left[\frac{V_o}{V_o + \Delta Q \Delta t} \right]^{b/\Delta Q} \quad [105]$$

The value of ΔQ is $Q_{in} - Q_o$. Time steps Δt are those chosen as appropriate for the solution of equation [100] above.

From the point of view of the various flow paths across the impoundment, given a variety of flow-entrance locations and outlet locations, the pond is actually a spatially lumped, fully mixed storage element as described. After the cessation of input to the pond, its settling and outflow are simulated until outflow ceases, with time steps chosen to optimise computations. The fact that the pond is on soil with a finite loss rate assures that outflow returns to zero at a reasonable time.

Simulation of Snow Budget

Precipitation records very rarely include data on whether the precipitation in winter periods occurs in the form of snow or rain. Further, since Opus is designed not to require detailed daily records of temperature, there is no way to accurately predict the occurrence of snow. Even when records of daily maximum and minimum temperatures accompany the precipitation record, often it cannot be ascertained whether a precipitation event was snow or rain. Thus the model for snow accumulation and melt in Opus is only approximate.

Accumulation of Snow In Opus, snow is assumed to be the precipitation form when the regenerated or measured sequence of daily maximum and minimum temperatures indicates that the mean daily temperature at the soil surface is less than 0°C . Snowpack is accumulated from any precipitation occurring as long as mean daily temperature remains below 0°C .

Simulation of Snowmelt Snow melt is calculated on days when a snowpack exists and when daily maximum temperature rises above 0. figure 26 illustrates the processes that Opus considers in estimating the melt and evaporation of snow. As with rainfall, a certain amount of snow is intercepted on any standing plant or dry matter. This intercepted snow is subject to early evaporation by available solar and thermal energy. Snowpack evaporation is calculated to be analogous to bare, wet soil evaporation, with PET obtained using the estimated albedo for snow-covered surfaces.

The daily effective melt temperature is apportioned for that part of the day that is estimated to have temperature above 0° C, assuming sinusoidal temperature variation. Melt is assumed to come from two potential heat sources; air heat convection and soil diffusive heat flux. Air heat melt is estimated using a degree-day method modified by shade and snow depth (Linsley *et al.* 1958). Snow depth is used as a simple surrogate for snow heat storage and ripening, which cannot be properly simulated without more detailed temperature information and heat transfer simulation within the snow cover. The Opus approximation of the effect of snowpack latent heat storage is illustrated in figure 27.

Melt due to soil heat flux is estimated whenever the surface soil temperature is greater than the assumed snow temperature (0°C). Transfer of heat from the soil to snow is assumed to be reduced by the presence of surface residue and mulch. The combined equation for estimating daily snowmelt potential (x_M , mm) is

$$x_M = \{4.5(1 - 0.4F_p^2)T_m c_f + 0.55T_{s2}\kappa_s(1 - F_m^2)\}\Delta t_m \quad [106]$$

in which

F_p	is relative shade cover over snow,
T_m	is effective melting temperature [$> 0^\circ\text{C}$],
Δt_m	is effective melt interval [days]
c_f	is the pack density factor = $0.5[1 + \exp(-.0005W_s^2)]$,
W_s	is the snowpack water equivalent, mm,
T_{s2}	is the soil temperature at 10mm depth,
κ_s	is the surface soil thermal conductivity [mcal/cm/sec/ $^\circ\text{C}$], and
F_m	is the relative mulch cover on the soil.

The first term on the right of Equation [106] is the degree-day estimate of melt from atmospheric heat, and the second term is the estimate due to thermal flux from the soil. The coefficient 4.5 is the degree-day melt coefficient (Linsley *et al.* 1958), and the second term coefficient is a units conversion factor. The term c_f (illustrated in figure 27) is the surrogate effect of the greater coldness of deeper snowpacks.

Estimated snowmelt water is added as surface input during calculation of the soil water flow, with a sinusoidal distribution during the day for days of melt. The amount that is estimated to be in excess of soil intake capability, when melt rate is high, is treated as runoff in the surface hydrology section of the model. When rain falls on a day when snow is melting, the two inputs are treated in sum.

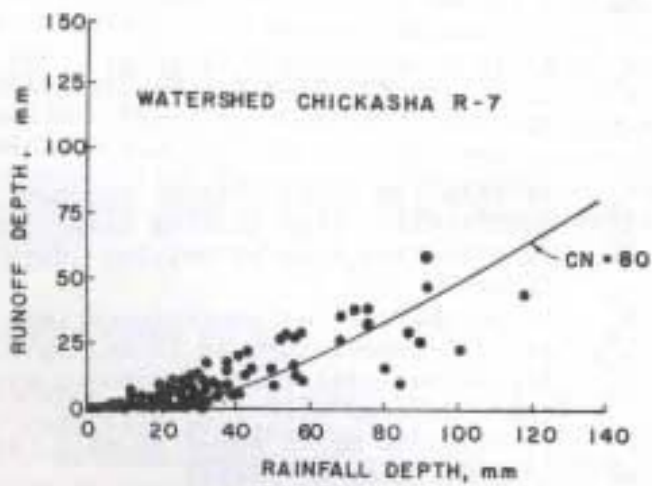
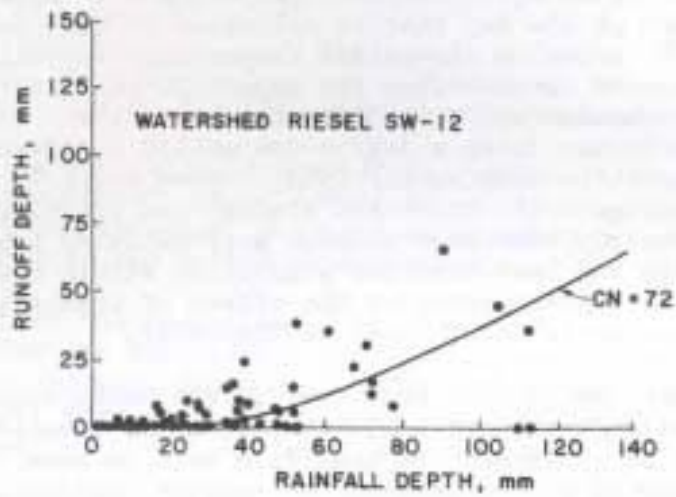


Figure 18.
Two examples of curve number relation compared with actual rainfall-runoff data. Measured daily rainfall and runoff, when plotted in this way, always show considerable scatter, which the more simple or lumped runoff relations cannot simulate accurately.

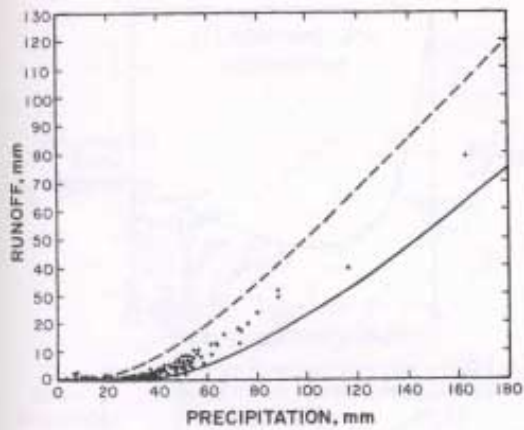


Figure 19. The SCS method for treating initial soil-water condition results in only a very small relative variation in predicted runoff. The two curves shown are the CN relations for antecedent conditions I and II. The case simulated is Watkinsville, GA.

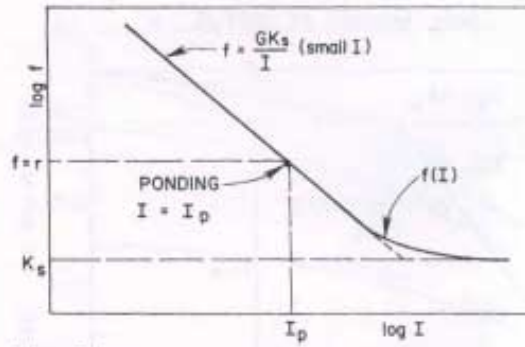


Figure 21. The Opus breadpoint hydrology relates infiltration capacity (f) to infiltrated depth (I). At short times this relation is an inverse one as shown. Actual infiltration rate is the smaller of f or rainfall rate (r). At larger times or at larger values of I , the relation becomes asymptotic to the constant K_s .

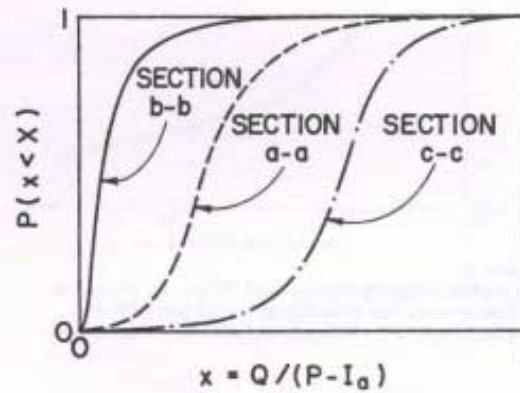
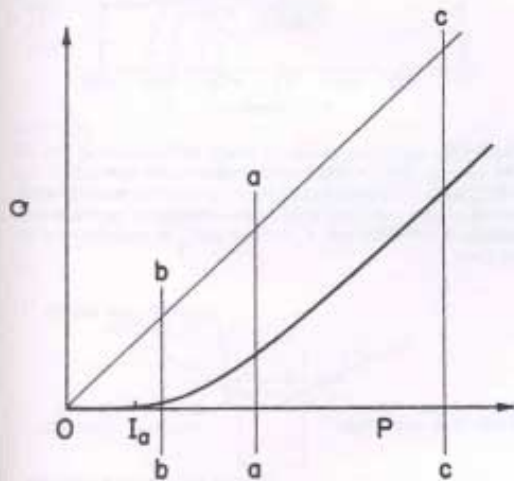


Figure 20. The probabilistic method in Opus assumes that the Curve Number method estimates an expected value of runoff. At any level of rain (P) in left figure (a, b, or c) there is actually a random distribution of runoff (Q). A two-parameter beta distribution can represent a reasonable distribution for relative runoff amount, as shown in the right figure.

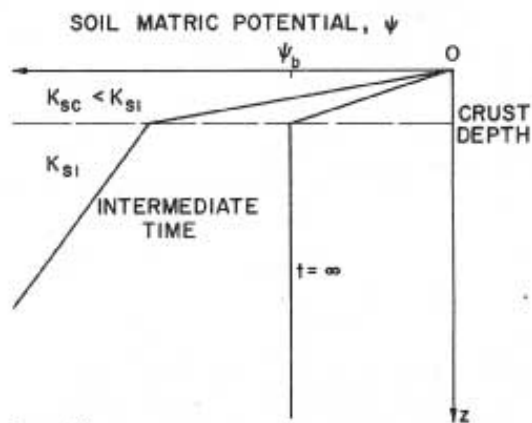


Figure 22. The effect of a surface soil crust on potential gradient in infiltrating soil. This effect is important in simulating the infiltration relation for the crusted soil case, which requires knowing the ultimate value of f .

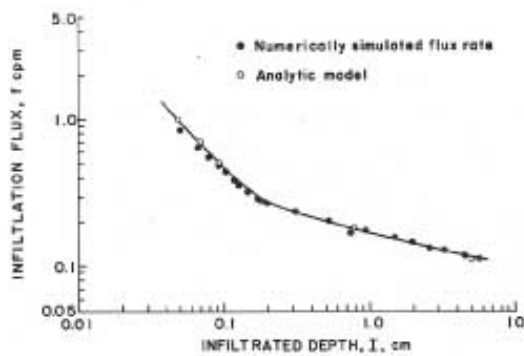


Figure 23. An analytic weighting method used in Opus for estimating infiltration in crusted soils. It is compared here with the numerical solution of Richards' equation for the same case.

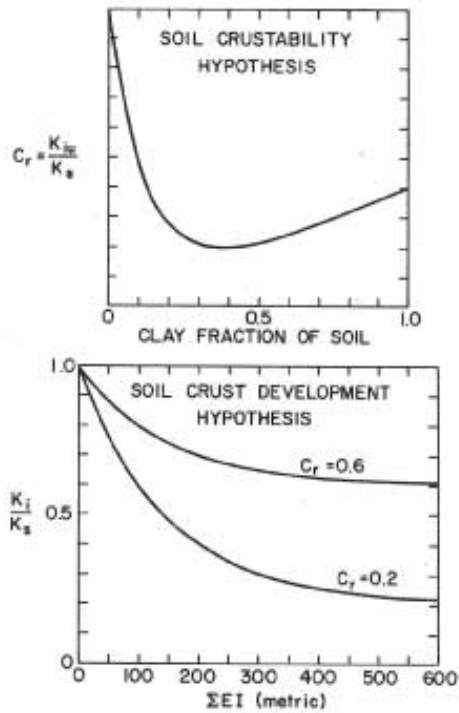


Figure 24. Two curves representing hypotheses used by Opus to estimate the relation between soil clay content, accumulated rainfall energy, and formation of restricted crust layers at the surface of cultivated soil. K_i is value of K_s in surface layer at any time.

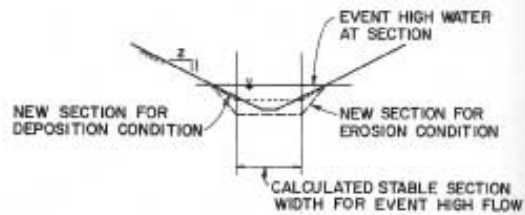


Figure 25. Section changes estimated by Opus based on an estimate of altered section bottom width for distribution of bottom shear. Erosion and sedimentation occur in different amounts at different locations along a channel or furrow, and cause changes in the furrow geometry.

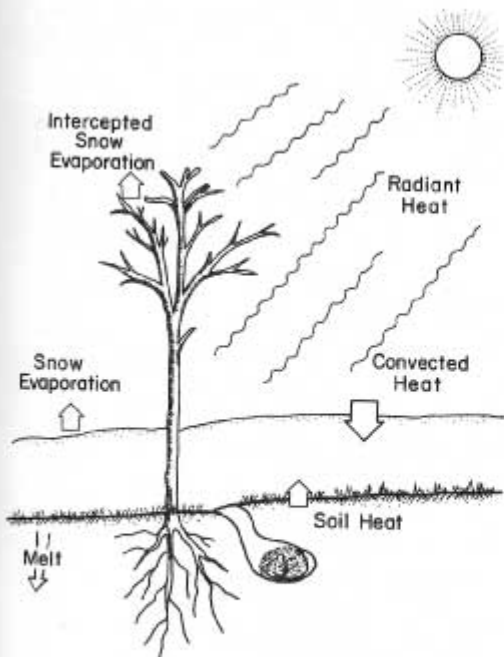


Figure 26.
 Various processes that affect snowmelt and snow evaporation. Snowmelt is assumed to include loss of intercepted snow from vegetation. Surface accumulations are melted from convective, radiative, and soil heat energy sources.

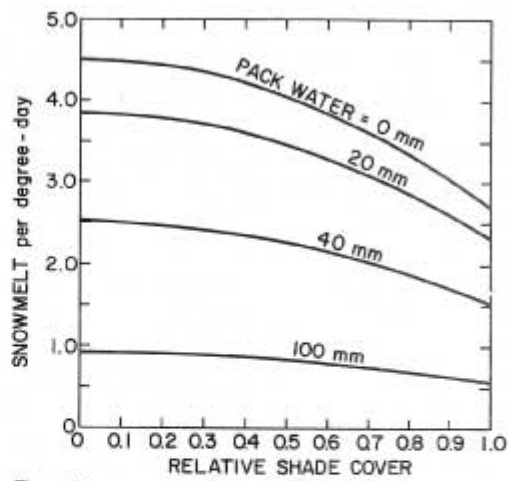


Figure 27.
 Opus approximation of effects of latent heat and shading on snowmelt.

6. Microbiological and Chemical Processes in Soil

Transformation of Nutrients

Because nutrients are a major contributor to agricultural nonpoint source pollution, it is important to simulate cycles of nutrients in the agricultural system as accurately as possible. These cycles describe the exchange of nutrients (including manures and fertilizers) between the plants, soil water, soil organic residue, and soil biota. Along with the transformation cycles of phosphorus, carbon, and nitrogen, the movement of all nutrients in tillage, mixing, and transport in soil water movement should be considered. All of these processes together determine the amount of movable material present at the surface when runoff occurs, and the amount leached below the reach of roots.

Organic matter is central to the cycling of plant nutrients, and the simulation of nutrient transformations in Opus is done by a version of the “Century” organic matter model of Parton *et al.* (1988b). This model simulates both labile and stabilized organic matter fractions, and thus simulates the nutrient-supplying capacity of the soil organic matter (SOM) as well as the local gains and losses of mobile nutrients. A more complete discussion of the modeling approach and the background for the Century model can be obtained from Parton *et al.* (1988b).

The nutrient model contains three SOM fractions (fig. 28), as follows:

- (a) An **active** SOM fraction of soil carbon (C), nitrogen (N), and phosphorus (P). This consists of live microbial matter and microbial products, along with partly humified soil organic matter with a short turnover time (1 to 5-y).
- (b) A **slow** SOM fraction of C, N, and P that is physically protected or more biologically resistant to decomposition. This fraction has an intermediate turnover time (20 to 40-y).
- (c) A **passive** SOM fraction that is chemically resistant and may also be physically protected from decomposition. This fraction has the longest turnover time (200 to 1500-y).

Plant residue (above and below ground) is divided into two fractions: **structural** carbon and nutrients, with 5 y turnover times; and **metabolic** carbon and nutrient pools that have 0.1 to 1-y turnover times. Decomposition products from these pools are transferred into the SOM pool described above.

Decomposition of each of the organic matter fractions is calculated using the following equation:

$$\frac{d(m_{rC})_i}{dt} = k_i f_w f_T (m_{rC})_i \quad [107]$$

where $(m_{rC})_i$ is the organic carbon in pool i [gm/m²],
 i is the pool index: 1 for structural,
 2 for metabolic surface litter,
 3 for structural soil residue,
 4 for metabolic soil residue,
 5, 6, and 7 for active, slow, and passive SOM.

t is time in days,
 k_i is decomposition rate coefficient for i^{th} pool,
 f_w is soil water content factor [figure 29], and
 f_T is soil temperature factor [figure 29].

The water content and temperature factors were developed based on laboratory and field observations (Parton, *et al.* 1987)

The decomposition rate parameters are constants except for k_1 and k_3 , which are functions of the lignin content of the structural material, and k_5 (the active SOM decay factor), which is a function of soil texture. Decay rates of surface litter are slower than those of soil litter, based on the assumption that soil moisture conditions are consistently less advantageous for surface material decomposition.

The model assumes that all pool transfers from carbon decomposition are a result of microbial activity and that microbial respiration is associated with each of these transfers. The relative amounts of loss of m_{rC} from respiration are shown in figure 28. The split of plant residue into structural and metabolic fractions as a function of the ratio of lignin (m_{rL}) to nitrogen (m_{rN}) was determined experimentally by incubation studies (Pinck *et al.* 1950). This split is determined using the following equation:

$$f_{rm} = 0.83 - 0.018 \left(\frac{m_{rL}}{m_{rN}} \right) \quad [108]$$

where f_{rm} is the fraction of residue that is metabolic. The fraction that is structural (f_{rs}) is $1 - f_{rm}$. The split occurs when the plant material is transferred into litter material or plowed into the soil and becomes residue. The fraction of structural material in the litter that is lignin (f_{rL}) affects the decomposition rate coefficients k_1 and k_3 in the following manner:

$$k_1 = k_{1c} \exp(-3f_{rL}) \quad [109]$$

$$k_3 = k_{3c} \exp(-3f_{rL}) \quad [110]$$

where k_{1c} and k_{3c} are appropriate constants. These relations cause the decay rates of structural material to decrease as relative lignin content increases. The relations are based on the assumption that the microbes can more easily decompose certain substrates when lignin contents are lower (Melillo *et al.* 1984). Values of parameters in equations [109] and [110] were obtained from laboratory incubation data.

Laboratory incubations were also used to determine functional forms for the effect of soil texture on decomposition (Sorensen 1981). Texture, in terms of sand fraction (f_S), is assumed to affect respiration efficiency (e_r) of the active SOM pool and its decay rate (k_5) as follows:

$$k_5 = k_{5c} (0.25 + 0.75f_S) \quad [111]$$

$$e_r = 0.17 + 0.68f_S \quad [112]$$

These relations have been verified by several studies (Parton *et al.* 1987). Determination of a value for k_7 could not be done by laboratory exercises but was found by observations on stable SOM levels at several sites and model tuning procedures (Parton *et al.* 1987)

The model operates on a daily time step, which is a modification of other versions of the Century model. Accumulations of added residue material and losses from crop harvesting and grazing are accounted for each day, when they occur. The location of the SOM pools is the top 200mm of soil, assumed to be the soil layer for active decomposition. Usually little residue decay takes place below this level, according to Parton. The mineral N pool is subject to transport through this zone with moving soil water. This is accomplished by the subsurface transport component of the model (Chapter 4). The model is linked to the plant growth component for uptake of mineral N and P and for input to litter of residue after senescence, or input of surface residue from plowing.

Nitrogen Submodel The nitrogen model has the same flow or state-transfer structure as the carbon model (see fig. 30). It is assumed that most N is bonded to carbon. Ratios of C/N for structural, active, slow, and passive pools are assumed to remain constant at a given site. The C/N ratios for structural and active SOM are set at 150 and 8, respectively, and the C/N ratio for slow and passive SOM is 11. These ratios are based on soil pedon analysis and other data (Parton *et al.* 1987) The n content of the metabolic pool is allowed to vary; any incoming plant N material not needed for structural C/N ratio goes to metabolic N. N transfers are stoichiometrically related to carbon transfers. Thus with the fixed C/N ratios, transfer between one pool and another during respiration can result in either immobilization or mineralization of N and/or P, depending on both the differences in C/N ratios of the pools, and the fraction of C lost as CO₂ during respiration.

Nitrogen may be added to the system as fertilizer mineral N, as plant residue N, or by biological fixation. Fertilizer N comes as an addition to either NO₃ or NH₄ in the surface layer, or a deeper layer in the case of injections. Urea is assumed very quickly transformed into NH₄ in the soil. Other N-transforming processes include fixation from the air and plant processes, and also denitrification and nitrification (Parton *et al.* 1988a). Daily fixation from atmospheric N (m_{NA}) is estimated by

$$m_{NA} = c_A + b_A(P_r) \quad [113]$$

in which c_A and b_A are fixed coefficients and P_r is daily precipitation. Fixation by nitrogen-fixing plants is assumed to occur to the extent necessary to prevent N-stress when necessary.

Nitrification, which changes NH₄-N to NO₃-N, is assumed to occur continuously in response to soil water content, temperature, and concentration of NH₄, as follows:

$$m_{Ni} = c_{Ni} f_W f_T f_{NH} \quad [114]$$

in which the f coefficients are predetermined factor functions of water, temperature, and NH₄ concentrations, respectively. The quantity c_{Ni} is a coefficient with a value of 0.1 for estimating m_{Ni} in gm/m²/day. Figure 31 illustrates the f functions used in equation [114]. Denitrification is modeled similarly, with an additional soil texture factor based on sand content. Denitrification causes mineral NO₃ to be volatilized in oxygen-poor situations. Oxygen poverty is usually associated with high water contents, and denitrification is thus approximated as follows (Parton *et al.* 1988b):

$$m_{Di} = c_{cn} f_W f_T f_{SN} NO_3 \quad [115]$$

with factors f similar to those for equation [114], but based on nitrate content (NO_3) rather than NH_4 concentration. The quantity f_{SN} is an approximator of texture and is defined as $4.66 - 4.8 f_s$, where f_s is the sand fraction. The coefficient c_{dn} is set and 0.0004. Figure 32 shows the factor f_w for the process. The factor f_T is the same as for nitrification. Units of m_{Di} are again in $\text{gm/m}^2/\text{day}$, with the computed amount being taken from the total NO_3 content of the upper 200 mm soil, and lost as gas. The amount of N volatilized is assumed to be 5 percent of the total N mineralization flows that accompany the decomposition of metabolic residue and SOM fractions.

Phosphorus Submodel The model for phosphorus (P) follows very closely that for N, with some small differences (figure 33) (Parton *et al*, 1988b) Ratios of C/P are used to trace P transformations that accompany C transformations between various pools. The primary mineral source of P is weathering of soil apatite. During weathering, labile P is taken up by organisms at the same time that secondary and occluded forms of P are produced (fig. 33). The SOM pools are assumed to have characteristic C/P ratios, and the amount of P moving between pools is determined, as for N flows, by the preservation of these ratios. Also as for N, P involved in respiration is assumed to be mineralized, and decomposition of structural residue (which is relatively low in N and P) is assumed to involve immobilization.

Degradation of Pesticides

As outlined below in Chapter 8, pesticides may be applied in several ways, and they enter the simulation after deposition on plants, surface soil, or on residue; or they may be incorporated directly into the soil at some depth. The portion of a pesticide on a plant surface is subject to both environmental degradation and washoff during rainfalls. Description of a pesticide in input data includes the fraction of plant adsorbed pesticide subject to washoff and also the first-order decay rate coefficient for this plant fraction.

Pesticides within the soil are assumed to be subject to environmental degradation or decay. The decay rate is modified by temperature and water content, since it is assumed to be strongly related to microbial activity. A first-order decay rate equation is assumed, with rate coefficient k_{ps} , as follows:

$$\frac{dm_p}{dt} = k_{\text{ps}} m_p \quad [116]$$

in which m_p is the local pesticide mass. The effects of water and temperature are assumed to be described by the Arrhenius equation (Walker 1974), as follows:

$$k_{\text{ps}} = k_{\text{psb}} f_w(\theta) \exp \left[\frac{b_{\text{ar}}}{1.99} \left(\frac{1}{T_{\text{Kb}}} - \frac{1}{T_{\text{K}}} \right) \right] \quad [117]$$

in which

T_{K}	is current Kelvin temperature,
T_{Kb}	is reference Kelvin temperature,
f_w	is a water content-activity function (see fig. 29),
b_{ar}	is a constant, and
k_{psb}	is decay coefficient and temperature T_{Kb} .

The coefficient b_{ar} is calibrated if data are given for a measured k_{psb} at a given temperature or water content, or else is assumed to have a default value taken from published values (Walker 1974). Without better and more widely available knowledge of the individual processes, Opus does not attempt to separate the various processes of environmental degradation and transformation of pesticides, such as hydrolysis and photochemical degradation). Since decay is assumed highly related to microbial action, it follows that a pesticide leached beyond the 200mm organically active depth will be decayed at a fraction of the rate in the active region. The user is allowed to select this fraction, or a default of 0.1 is used. Degradation rates even within the active zone are made a function of soil layer relative organic matter content, so knowledge of soil organic matter is important for pesticide simulations.

Pickup of Chemicals by Runoff

The movement of both soil and surface water is involved in the transport of chemicals in the agricultural environment. However, the occurrence of a runoff-producing rain has the primary role in actually moving chemicals off the field. Nonrunoff rainfall events can also move chemicals from plant and surface residue into the soil surface.

Opus simulates several processes that cause chemicals in runoff water. The methods are designed to operate with both hydrology/erosion options provided. This dictates that the methods are lumped, although it is possible to simulate the processes more realistically as dynamic, distributed transport as for the sediment option for 'breakpoint' rainfall hydrology. One can argue, however, that more detailed distributed calculations have limited reliability because of the many uncertainties and approximations in other parts of the model.

The following paragraphs outline the methods used in Opus to estimate the loads of nutrients and pesticides in runoff water, and the amount of each that washes into the soil from the surface during rainfall. These constituents are treated identically, with a few noted exceptions. The following discussion uses labile phosphorus, P, as an example.

Leaching of Chemicals from a Plant Canopy For all rainfalls that exceed the interception storage of the current canopy cover, a certain small fraction of the N and P contained in the plant, or washable pesticide from its surface, is assumed to wash off the plant with the rainwater. For living plants, this fraction is assumed to be 0.02; for standing residue, or plants undergoing senescence, it is assumed to be 0.03 (Schrieber 1990). If the period since the last rainfall or washing event [Δt_d , days] is greater than 1, the fraction is reduced by a factor f_{pw} as follows:

$$f_{pw} = 1 - \exp(-6\Delta t_d) \quad [118]$$

In addition, the amount leached from a plant is proportional to the percent cover that the crop represents compared to the field surface (F_p). Thus the estimated field value of P leached from the canopy [m_{pcL} , kg/ha] is

$$m_{pcL} = 0.02m_{pc} f_{pw} \frac{F_L}{F_{LT}} \quad [119]$$

in which m_{pc} is P content in (or on) crop 'c' [kg/ha],
 F_L is leaf area index for crop 'c', and

F_{LT} is total field leaf area index, considering all plants.

Leaching of Surface Residue Rainwater also leaches decomposition-product nutrients from residue on the soil surface. This process is assumed to be similar to the clarification of a simple reservoir. Adding water to a solution in an overflowing reservoir results in exponential decay of concentration, assuming a fixed mixing efficiency. The leaching constant for residue is assumed to be 0.05 per mm of rainfall. The amount of P in the residue that is leached in a given storm [$m_p(rs)$] is assumed (re Schrieber 1990) to be

$$m_p(rs) = m_p(rs) (1 - \exp[-.05V_p]) \quad [120]$$

where V_p is the rainfall passing through the residue and $m_p(rs)$ is the mass of P in the residue (kg/ha).

Routing Chemicals in Infiltration and Runoff

A chemical from the above sources (plus nitrate in rainwater) will either enter the soil or leave the catchment in runoff. The path of a solute is estimated according to the division of rainfall in the infiltration process. For either hydrology option, the first part of the rainwater will all enter the soil. This portion, I_p , is then distributed downward from the soil surface along with any dissolved chemicals to the depth reached by the wetting front at ponding, or the beginning of runoff. A more realistic model for this process for rainfall intensity simulation has been made by Havis *et al* (19). The approach here is necessarily lumped.

Rainfall and washed solutes reaching the soil surface after the beginning of runoff will be divided between infiltration and runoff, but all incoming rain will interact with the flowing surface water. The concentration of chemicals in the upper soil layer, assumed to be interactive with the runoff, is calculated at the time runoff begins, based on the amount I_p , which has washed through it. Then the rainwater that exceeds I_p interacts with this surface zone as a simple reservoir during runoff. For chemicals such as P and NH_4 , this interaction assumes the behavior of an equilibrium adsorption isotherm. The depth of the interactive soil is related to soil disturbance, porosity, and infiltration characteristics. The user is asked to specify a fraction (f_z) of the 10mm upper computational layer as the active depth.

The mixing interaction is assumed similar to that in soil water transport. The estimated runoff water concentration (C_{ro}) is

$$C_{ro} = C_{Pi} + (C_{Po} - C_{Pi})F_e(r_e, M_w) \quad [121]$$

in which C_{Pi} is P in water reaching surface after runoff begins,
 C_{Po} is P concentration in active soil zone at beginning of runoff,
 F_e is $(M_w/r_e)[1 - \exp(-r_e/M_w)]$

In this expression, M_w is the total equivalent water depth (mm) for the active layer for chemical P, (were it all dissolved):

$$M_w = 10\theta_1 + 1000K_{dP} M_1$$

in which θ_1 and M_1 are the water content and mass of the upper layer, respectively, and K_{dP} is the adsorption coefficient of chemical P.

Finally, the amount of P in the runoff is assumed to equilibrate with the transported sediment, if any, according to the equilibrium adsorptivity described by K_{dP} , which partitions the P in runoff between that adsorbed and that in solution.

Pesticides enter runoff water by the above mechanism, but for pesticides, plant washoff is not presumed to enter the soil from runoff, but soil incorporated pesticides may interact with runoff water. When kinetic adsorption dynamics are chosen, the equilibrium assumptions of equations [121] and [122] cannot hold correctly. An estimate is first made of the average concentration of the dissolved and the adsorbed amounts of each chemical in the upper layer during runoff time. A weighted average is used. The weighting is proportional to the ratio of infiltrated water to the water content of the upper layer. More infiltrated water will more heavily weight the concentrations at the end of the runoff event. Then the pesticide is assumed to interact with the runoff water, using a surface active fraction as above, and assuming a reduced equilibrium mass fraction based on the kinetic rate factor (v) and length of rainfall (t_r) as follows:

$$f_b = \exp[t_r(0.01 - v)] \quad [123]$$

The factor f_b is multiplied by the surface interactive fraction (f_z) to obtain the equivalent amount of soil from which the adsorbed pesticide will equilibrate with the runoff water. For the equilibrium option, f_b is 1. The total chemical from the soil available for interaction (M_{Pt}) is then

$$M_{Pt} = f_z[M_{Ps} + f_b C_a M_1] \quad [124]$$

where M_{Ps} is the mass of pesticide in soil solution in the upper layer, and C_a is the adsorbed concentration of chemical P.

Writing an equation for this amount equilibrated with the total runoff water depth Q (mm) m and solving for the concentration of runoff dissolved pesticide (C_{ro}), one obtains

$$C_{ro} = \frac{M_{Pt}}{\frac{1}{c_h} + f_z f_b M_1 K_d} \quad [125]$$

in which c_h is the conversion factor, defined below equation [37]. The amount of chemical P dissolved in runoff in kg/ha is the concentration times Q divided by the conversion factor c_h . The concentration of chemical on sediment (C_{pm}) results from surface soil that has released pesticide into runoff, according to fraction f_b , plus the adsorbed material on transported surface soil, as follows:

$$C_{pm} = K_d C_{ro} f_b + (1 - f_b) C_a \quad [126]$$

where C_a refers to effective surface soil-adsorbed concentration during the runoff event, as discussed above. This concentration is then multiplied by the enrichment ratio and the sediment mass to obtain the estimated amount of each chemical that leaves the catchment on

sediment. The amounts adsorbed and dissolved in the surface soil are then adjusted for this loss by mass balance.

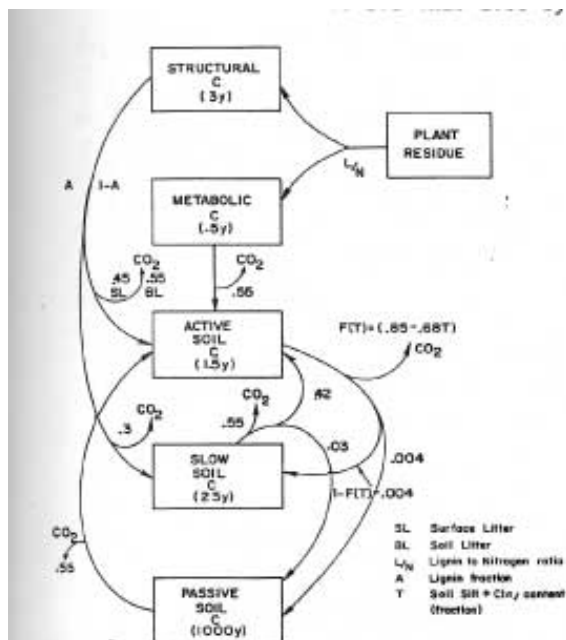


Figure 28. Diagram for the century model of the organic carbon cycle (used in Opus) and the flow of carbon between the various pools. (Reproduced with permission from Parton et al. 1988b.)

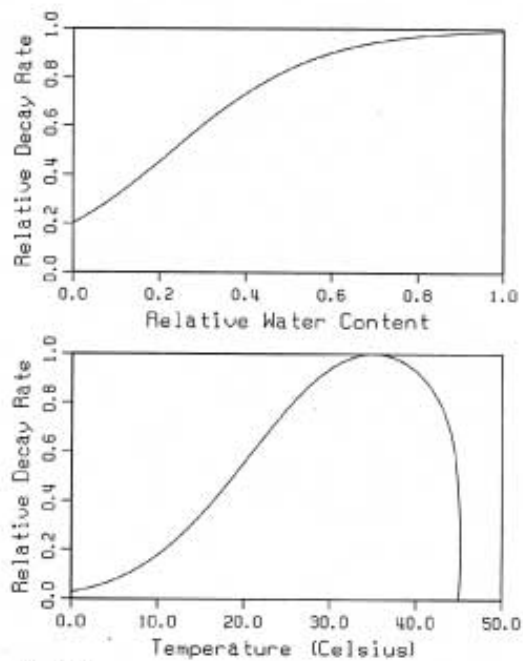


Figure 29. Relative effect of soil moisture (top) and soil temperature (bottom) on microbial decay process for the Century model for soil carbon and nutrient cycles.

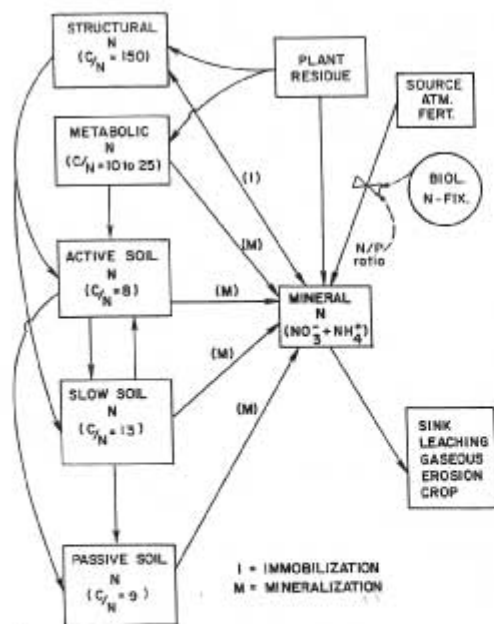


Figure 30. Diagram for the Century model for organic nitrogen cycle and the flow paths for exchange of N between pools. (Modified from Parton et al. 1988b.)

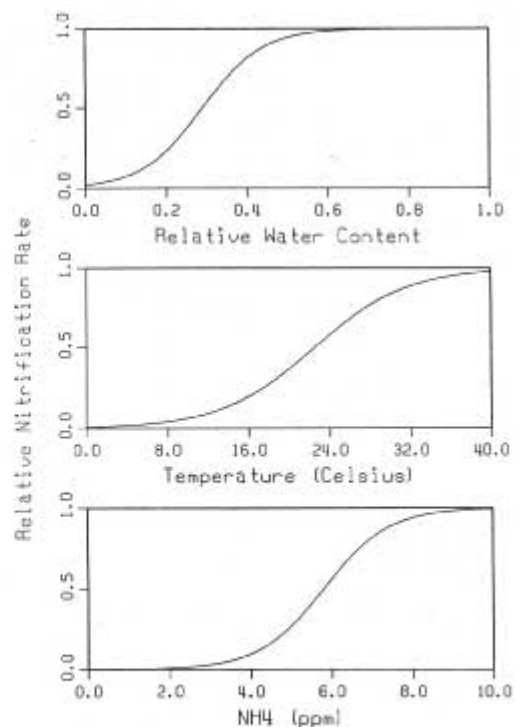


Figure 31. Functions for the effects of the soil water content (upper), soil temperature (middle), and soil ammonia (lower) on relative rates of nitrification.

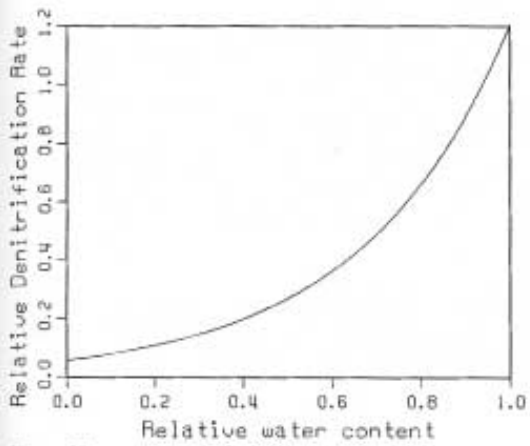


Figure 32.
Relative effect of water content on rate of denitrification in the Century model for nitrogen cycling.

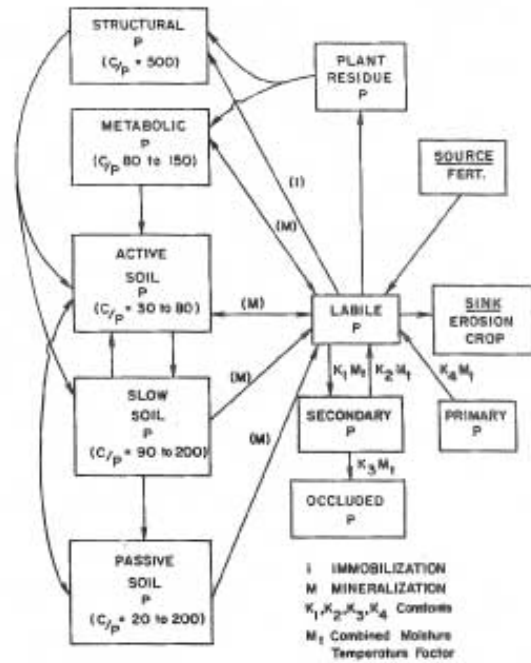


Figure 33.
Diagram for flows between various pools in the Century model for phosphorus in Opus. (Reproduced with permission from Parton et al. 1988b.)

7. Simulation of Plant Growth

Opus uses a mechanistic plant model to simulate the growth and development of plants or crops in response to the four major environmental factors: radiation, nutrients, temperature, and water availability. The model may be used for either annual or perennial plants, and it responds to stresses, grazing, and harvest in a relatively realistic manner. It is similar and related to the plant-growth method in the EPIC model (Williams *et al.* 1984), since many of the Opus plant model features were inspired by early versions of the EPIC plant model.

Growth Model

In general, the plant model can be expressed as a growth equation for incremental addition of plant material, (Δpm), modified by several factors:

$$\frac{\Delta pm}{\Delta t} = c_e f_e f_a f_m \phi R_i \quad [127]$$

in which

- c_e is a coefficient representing photosynthetic efficiency [kg/ha/langley],
- f_e is a factor (0 to 1) for relative leaf area [F_L] capture of radiation,
- f_a is a age-limiting (senescence) cutoff factor,
- f_m is a mass-limiting cutoff factor,
- ϕ is a stress factor for growth-limiting stress(nutrients, temperature, water),
- R_i is daily radiation input [langleys].

The value c_e is time invariant, but is crop-related, and varies over a limited range. The values f_a and f_m are functions of plant thermal age in degree-days, and total size in kg/ha, respectively. They auto-regulate the plant growth when maximum age or size is approached. Their functional form is shown in figure 34. These functions are mechanistic and conceptual rather than experimentally or physiologically determined, but they produce a plant response that imitates observed plant behavior.

Self-Dependent Growth The value f_e reflects change over time in the plant's ability to intercept radiation and photosynthesize new material as the leaf area increases toward that at leaf maturity. Growth depends on the amount of radiation that can be intercepted by the leaves and thus on the active leaf area. The relation of leaf area index (F_L) to leaf mass is discussed below. Because of shading and the variable nature of maximum F_L (referred to here as F_{LM}), the relation of f_e to F_L/F_{LM} is direct at small values of F_L , but is asymptotic to and upper limit of 1. The equation used, illustrated in figure 35, is

$$f_e = 1 - \exp\left[\frac{-3F_L}{F_{LM}} - v_e - c_i\right] \quad [128]$$

parameters v_e and c_i are two modifying factors. Factor v_e is employed when, as in perennial plants, the root mass is large relative to aboveground mass, and stored energy can be used to produce leaves and plant material more quickly. It is defined more precisely below. Factor c_i is similar but represents the initial energy available in some seeds to produce seedlings without leaves yet present. These two factors are zero when not applicable. Factor c_i is mathematically necessary to initiate plant growth, just as factors f_a and f_m are necessary to limit growth. In

mathematical terms, equation [127] is a modified linear differential equation, at least at small values of pm, and could not exhibit growth at pm=0 without a positive value of c_i .

As leaf area increases, growth rate can increase, expressing a self-dependent growth rate. The parameter on the curves in figure 35 indicates the simulated effect of excess root/leaf ratio. The value of ve is the ratio of mass of roots to mass of stems+leaves in excess of that which is normal for the total plant mass. Positive values of ve can occur under hay or early alfalfa harvest, for example, or for grazing loss of above-ground plant material. This ratio also expresses an early spring start for perennials with an established root system, compared with plants starting from seed. A value of $ve = 0$ indicates normal root/leaf ratio for annuals.

Growth-Limiting Stresses The stress factor (ϕ) is the minimum of individually evaluated stress-coefficient values for water availability, temperature, and nutrients. The range of values of all those coefficients is 0 to 1, with 1 being a value of no stress. These values are each evaluated each day, and ϕ is assigned the value for that stress factor that is minimum.

Water Stress: The water stress factor is based on the soil water found within the root zone for a crop. Thus it depends in part on the depth of roots. It is evaluated by summing all the available water in the soil of the root zone, considering water pressure head. The user may specify a critical soil pressure head, ψ_c , (or a default may be used), giving an associated water content θ_c , below which water availability declines linearly to zero at wilting point head, ψ_w (and water content θ_w). The available water, W_a , is found by summing the available water content, θ_a , times each depth increment Δz , with θ_a found as follows:

$$\begin{array}{ll} \theta_a = \theta & : \quad \theta \geq \theta_c \\ \theta_a = 0.5*(\theta + \theta_w) & : \quad \theta_c > \theta > \theta_w \\ \theta_a = 0. & : \quad \theta_w \geq \theta \end{array} \quad [129]$$

Water stress ϕ_w , is calculated as the ratio of W_a to the plant potential transpiration (each in mm), or 1.0, whichever is the smaller

Nutrient Uptake and Stress The nutrient stress factor (ϕ_N) is a function of the ratio of actual to potential use of plant nitrogen. Phosphorus stress is not simulated, and plants are assumed to maintain a given N/P ratio, which is used in the residue decay model (chapter 6). Potential use of plant N is obtained from information on the N content of the plant at a certain growth size, as illustrated in figure 36. Plants typically contain more N at emergence than at maturity. The relation of fractional N content, n , to relative size, d , is expressed as an exponential function of relative size, with 3 parameters:

$$n(d) = n_m + (n_o - n_m)\exp(-c_d d) \quad [130]$$

in which d is relative plant size as a ratio of dry matter, pm, to potential maximum dry matter, ppm.
 n_o is plant fractional N content at emergence,
 n_m is plant fractional N content at maturity,
 c_d is a shape coefficient.

This allows estimation of the potential content of plant N at any age. If root-zone soil N is insufficient to meet the daily N demand thus estimated, the N stress factor is calculated as:

$$\phi_N = 2 \frac{\text{actual N use}}{\text{potential N use}} - 1 \quad [131]$$

It is assumed that plant roots are able to selectively garner nitrogen from soil water if the N demand by the plant exceeds that amount present in the daily water uptake. Plant use cannot exceed the nitrate and ammonia in the soil water ambient to the roots.

Temperature Stress The plant temperature stress factor, ϕ_T , is a dimensionless function of the daily mean air temperature, T , the minimum growth temperature, T_b , and the optimum growth temperature, T_{op} . The last two values are plant specific parameters, and the function using these parameters is illustrated in figure 37. Several types of curve functions are candidates to represent observed plant temperature responses, and plants naturally differ somewhat. The ϕ_T function (as well as other stress functions, for that matter) used in Opus may not exactly represent every type of plant. The normalized temperature T^* used in figure 37 is defined on the abscissa.

Allocation of Plant Material Plant material produced by the model thus described is divided among leaf/stalk, root, and fruit/seed categories according to the plant's relative age and size. A general division function is presently used for all plants, and is illustrated in figure 38. Relative root/leaf ratio is a function of relative mass (lower scale), and relative seed or fruit material allocation is a function of relative age in degree-days (upper scale). The age when the plant begins producing fruit/seed is user selectable, and defaults at 0.5.

The plant material in leaves and roots must be interpreted to estimate leaf area index (F_L) and rooting depth to complete the plant description. The relation between the mass of plant material in leaves/stems (pm_{lv}) and F_L is assumed to follow a nonlinear function as follows:

$$F_L = F_{LM} \sin \left[\frac{\pi}{2} \frac{pm_{lv}}{ppm_{lv}} \right] \quad [132]$$

in which F_{LM} is the potential maximum plant leaf area index, and ppm_{lv} is the maximum potential leaf/stem dry matter in kg/ha. (a plant parameter). The plant material allocated to root mass (pm_r) results in a gradual increase in depth of root penetration into the soil, Z_r [mm], up to a maximum value, Z_{pr} , as follows:

$$Z_r = 10 + (Z_{pr} - 10) \left\{ 1 - \exp \left[-2 \left\langle \exp \left(1.5 \frac{pm_r}{ppm_r} \right) - 1 \right\rangle \right] \right\} \quad [133]$$

in which ppm_r is the potential maximum root mass for the plant.

Interaction of Plant Growth Factors

If the leaf-intercept area were directly proportional to plant dry matter and if the age and senescence factors are ignored, equation [127] would be a linear differential equation. Growth could not initiate without the presence of c_i , as said above, which may be thought of as representing the ability of the plant to produce leaves from seed material. As described above, the plant material produced is divided between root and nonroot material. If we assume for the moment that factors f_a , f_m , and R_i are constants, and the f_e is proportional to F_L plus the value c_i

(as is true at small F_L), the equations [132] and [133] can be combined and simplified to illustrate the basic growth-rate function as:

$$\frac{dM_*}{dt} = B[\sin(M_*) + b] \quad [134]$$

in which M_* is $\pi/(pm/ppm)$,
 B is $\pi/2(Y/ppm)$
 b is c_i/Y
 Y is $f_a f_m R_i c_e$.

The solution of equation [134] has the form

$$t = \frac{1}{Bv} \ln \left[\frac{b \tan(M_* / 2) + 1 - v}{b \tan(M_* / 2) + 1 + v} \right] \frac{1 + v}{1 - v} \quad [135]$$

in which $v = \sqrt{1 - b^2}$.

Although equation [135] includes assumptions neglecting senescence factors, it can help obtain an index of the optimum time to maturity for a set of plant parameters, by solving for t when M_* reaches its peak of $\pi/2$. Notice that although the solution is scaled, the time is inversely proportional to B and is thus proportional to ppm. This is reasonable because a fixed amount of radiant energy is available, which causes larger plants to reach maturity at later dates than small ones, all other factors being equal.

Senescence After maturity, failing a harvest operation that removes the plant, active leaves will turn to “standing dry matter” at a rate specified as a parameter by the user. Roots of annual plants are converted to soil residue when active leaf area falls to zero. For perennial plants, roots are assumed to recycle and regenerate 10 percent of their mass over winter. No doubt this figure actually varies widely with plant type and climate.

In summary, the major parameters needed by the model to describe a plant include the following:

- (a) seasonal lifetime in degree-days to onset of senescence.
- (b) age in degree days at emergence. These two values are measured from the crop year start for perennials, and measured from the day of planting for annuals.
- (c) potential production of total plant material (and fruit) for unstressed conditions [ppm]
- (d) N content with growth stage (three parameters)
- (e) maximum depth of rooting,
- (f) maximum leaf area index, and
- (g) conversion efficiency for turning radiation into plant material

Discussion Like some other parts of the Opus model, the plant growth model is well behaved (or at least bounded in its response to inputs), but also is difficult to exhaustively test because of the paucity of data on the growth response of plants to known amounts of stress. Data exist for only a few crops with simultaneous measures of plant mass, leaf area, soil water content, and nitrogen available in the root zone. Typically, experimental objectives are limited to only a few of the possible stress factors. The model described above has been exercised against various

types of plant data from several climates around the continental United States, and parameters found have been given in the User manual (vol. 2). That tabulation should help a model user in estimating values for related crops and climate zones. There is no substitute however, for a user having a good idea of what a crop growth pattern should be, and adjusting appropriate parameters until the plant behaves reasonably.

Examples of Plant Growth Simulation

Figure 39 illustrates the plant model simulation of a hypothetical corn crop. For this figure, no stresses were assumed. The combined action of the factors f_e , f_m , and f_a is manifest in the shape and timing of the growth pattern that results. The same corn parameter set produces significantly less when the stresses of limited water and nutrients are included, as illustrated in figure 40. This particular year, 1973, was a relatively dry one at the site of the corn being simulated. Application of the plant model to a multiple harvest grass (or hay) field crop type is illustrated in figure 41.

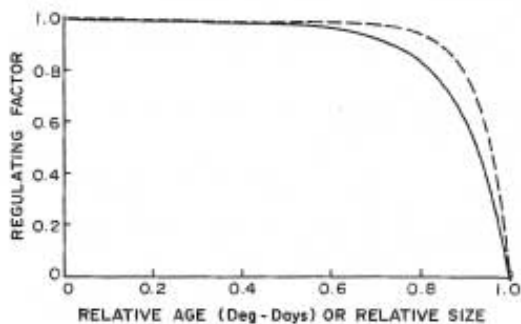


Figure 34. The relative growth factors f_e and f_m , representing relative aging and relative size used in the mechanistic plant model.

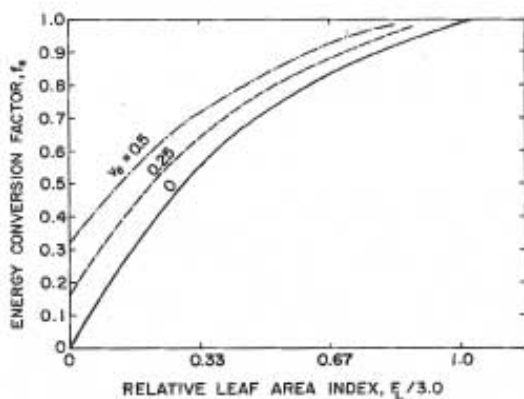


Figure 35. Illustration of equation [128]. As leaf area index increases, the relative ability of the plant to intercept radiation and produce new plant material increases at a decreasing rate, with an upper limit of 1. For perennial plants or cropped grasses, energy stored in roots can effectively increase this rate; V_r is relative proportion of roots to aboveground material in excess of normal ratio.

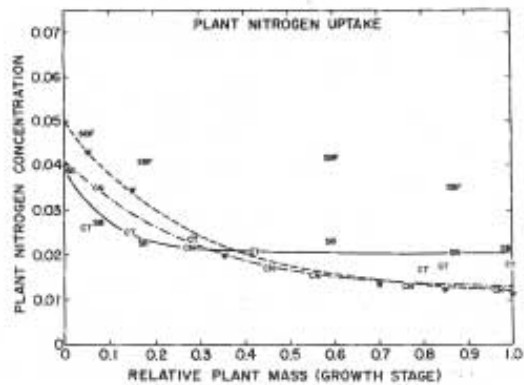


Figure 36. Concentration of plant nitrogen as a function of relative size or growth stage for several common crops. Symbols are from published data: W = wheat (Boatwright and Haas 1961), CN = corn (Hanaway 1962), SB = soybeans (Hanaway and Weber 1971), SBF = fertilized soybeans (Hanaway and Weber 1971), CT = cotton (Bassett et al. 1970).

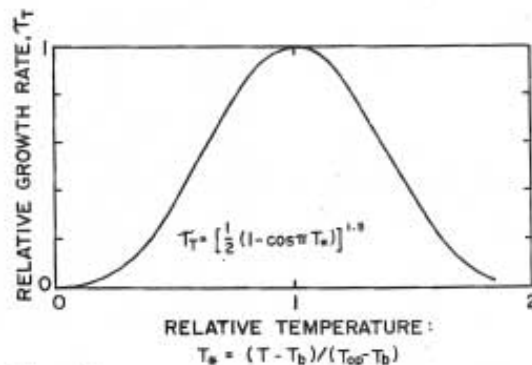


Figure 37. Relative effect of temperature on growth rate of plants, based on a scaled or relative temperature. T_b is lowest and T_{op} is optimum temperature for plant growth.

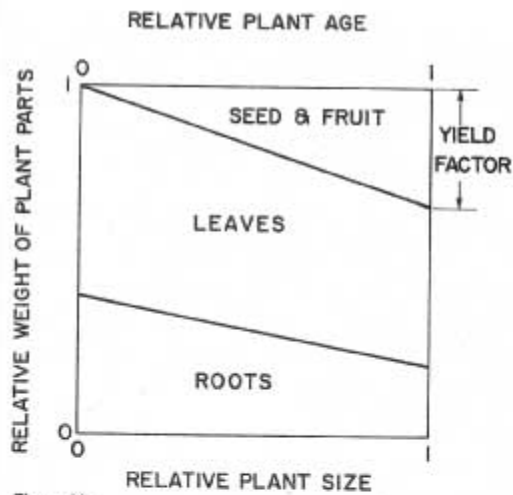


Figure 38. Division of plant material by the plant growth model in Opus. Plant material produced by the plant is divided between leaves, roots, and fruit according to the relative size of the plant or the relative age of the plant (upper scale) in the case of fruit.

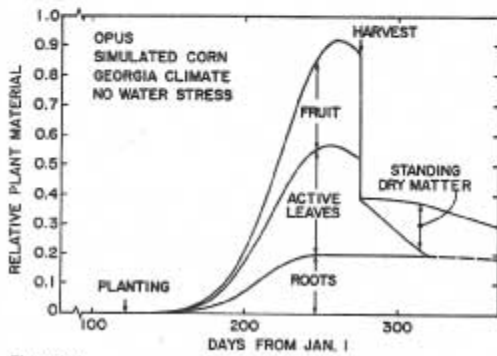


Figure 39. Plant model simulation of ideal growth (no stress) of a corn crop in Georgia.

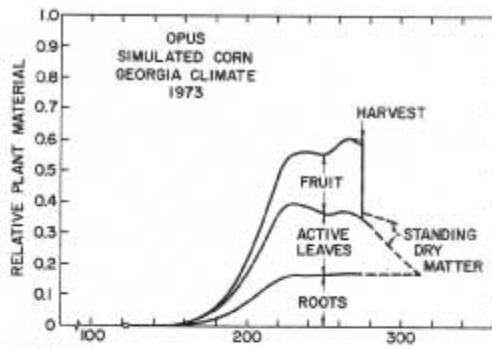


Figure 40. The same simulation as in figure 39 except that water stress was included, reducing growth and yield.

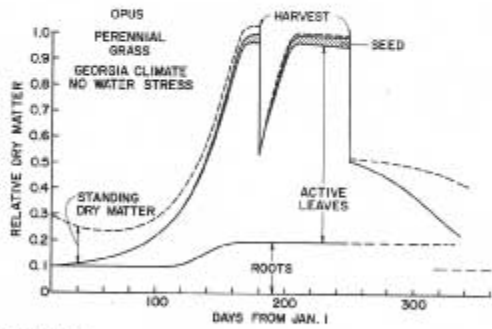


Figure 41. Example Opus plant model simulation of the growth of a multiply harvested grass crop. This figure illustrates the rapid regrowth feature where root resources are available.

8. Specifying Management Operations

Several major options for the use and treatment of land are specified as part of the field description, discussed in chapter 2. These include the direction of tillage and the use of terracing, impoundments, and grass buffer strips. Other management operations which make changes in the plant or surface conditions, are discussed below. Management is assumed to occur on a rotation basis, with the rotation cycle up to 5 years long and repeated as often as necessary to cover the simulation time.

Management operations are specified by a list of operations, including whatever parameters necessary to describe the management effects, plus a schedule that specifies the time and other variables pertaining to application. The list contents define the operation, depending on the type of operation – fertilization, plowing, spraying, for example. The schedule specifies the date but also any variable amount, e.g. fertilizer applied. For example the pesticide list describes the chemical characteristics of each chemical, and the schedule gives the date and application method. Each year in the rotation cycle has a schedule, but there is only one list for each type of operation. Lists must be given for chemicals used, tillages, manures, and plant types (growth model parameters).

Lists of Choices

Opus allows users to choose from among crops to grow, tillage procedures to use, pesticides to employ, and manures. Certain characteristics of members of these four lists are specified and remain constant, independent of application date or application method.

List of Crops The set of parameters representing a crop or plant (as given in chapter 7) are listed for each plant species that is grown during the simulation. For a perennial, a mix of perennials, or an unmanaged catchment, the rotation period is 1 year. A maximum of four plant species may be treated simultaneously, i.e., found growing at the same time. When an annual is planted, the parameters in this list are used by the plant model to simulate its growth. The crop parameter list includes specification of a type for each plant. The types available are: annual, harvested perennial, grazed perennial, annual grazed meadow, and tropical perennial (no senescence). The type code controls how the plant model operates with regard to certain options, such as root renewal, and how other instructions are interpreted. These features are fully explained in the User's Manual.

List of Mechanical Operations Mechanical operations in the field are classed into four types, numbered as follows:

1. **Planting** A plant seed or seedling is placed in the ground, during which operation some soil mixing may also occur, and row spacing is specified. The row spacing should not be changed until after harvest. Planting “degree-day” timers are started.
2. **Cultivation** The field soil is disturbed with a specified mixing efficiency to a specified depth. Growing or standing dry plant material is not disturbed, and row spacing is unchanged. Furrow depths may change, and surface material may be mixed into the soil to a specified efficiency and depth. These limitations distinguish *cultivation* from *plowing*, described below.
3. **Harvesting** A specified proportion of the plant is removed, including at least the seed/fruit portion, but optionally also some of the other above ground material. The soil is not mixed, and furrows are unchanged. A special code allows harvesting of the roots for root

crops. For grazing operations, a special code allows this data to be used to specify a grazing rotation for removal of plant leaves and stems at a given rate for a given number of days.

4. **Plowing** Characteristics are similar to cultivation, except that plant material on the surface is not excluded, row spacing and furrow depths may be changed as well.

Data for operations type 1 and 3 must include the naming of the crop to be planted or harvested. Mixing that accompanies operations type 1,2, and 4 causes major changes in the surface soil material. Soil bulk density is returned to a minimum value, surface crusts are destroyed, and soil water and dissolved and adsorbed chemicals are partially mixed over the depth specified. This includes surface mulch and plant residue (except growing crops for type 2). It is assumed that plowing or cultivation does not extend deeper than the 200mm active surface soil zone, and the nutrient pool values are not changed. Because of this mixing, Opus will not properly treat a soil horizon that is shallower than 200mm.

List of Pesticides The characteristics of all pesticides to be used during the simulation period are specified in a list. This includes decay rate constants, solubility, adsorption coefficients (as K_{oc}), washability of portions on plants, and Arrhenius constant if known.

List of animal Wastes Each manure that is applied during a simulation is described in a parameter list. Opus includes a default list of 9 common manure types, giving data on percent organic matter, total N content, ammonia N, and phosphorus. Any of these nine may be altered, and a tenth may be created by the user. Inorganic fertilizers are more simple, and are specified along with the schedule in terms of their content of NO_3 , NH_4 , and P in kg/ha.

Schedule of Operations

The lists above are for the fixed characteristics for operations that may be repeated several times, or for the characteristics of a plant or chemical that are fixed. Variable aspects of operations are given in the operations schedule. There are separate schedules given for each rotation year for mechanical operations, fertilizations, pesticide applications, and irrigations. There may be as many as 5 years in the cycle. For the northern hemisphere, the farming calendar is assumed to start on January 1, and all schedules must present the operations in order. For the southern hemisphere, the calendar begins on July 1, and operations must be listed in order from July through June 30 of the following year.

The schedules needed include the following:

- (a) Tillages (mechanical operations) are specified by the number from the tillage list, and by date of implementation.
- (b) Fertilizations are specified by date plus rate of application for each of nitrate, ammonia, and phosphorus. In addition, if animal wastes are applied, the number from the manures list is given, and an application type is specified, including injection, with liquid, etc.
- (c) Pesticides are applied by specifying the number from the pesticides list, and application type, and an application rate (kg/ha or lb/ac)
- (d) Irrigations schedules include the type of irrigation (sprinkler, flood, border, etc.), the amount of application, and the schedule method (every n days, as needed, or a list of particular dates).

There are four types of irrigation types allowed: sprinkling based on a soil water deficit level, furrow based on deficit, furrow or level basin from a ditch (every n days), and level basin with

dates individually specified. The ditch supply option assumes irrigation from a ditch system that requires irrigation on a fixed management schedule. For sprinkler irrigation, it is assumed that the rate of application is properly set so that runoff does not occur and need to be simulated.

Each fertilization can apply any or all of the nutrient types. Any of the various operations can occur on the same day. One fertilization option is that dissolved N may be applied with irrigation. In that case, the operation days must coincide when that application is so coded. Another control is the state of the field: the user can specify a water content above which the field is assumed too wet for any mechanical operation, and it will be delayed until that wetness threshold is satisfied. The User Manual contains more specific information on how various operations are to be indicated in the parameter file.